


















Where the “*ruber*” Meets the Road: Using the Genome of the Red Diamond Rattlesnake to Unravel the Evolutionary Processes Driving Venom Evolution

Samuel R. Hirst ^{1,*}, Rhett M. Rautsaw ^{1,2}, Cameron M. VanHorn ¹, Marc A. Beer ², Preston J. McDonald ¹, Ramsés Alejandro Rosales García ³, Bruno Rodriguez Lopez ⁴, Alexandra Rubio Rincón ⁴, Hector Franz Chávez ⁵, Víctor Vásquez-Cruz ^{6,7}, Alfonso Kelly Hernández ⁷, Andrew Storfer ², Miguel Borja ⁴, Gamaliel Castañeda-Gaytán ⁴, Paul B. Frandsen ⁸, Christopher L. Parkinson ³, Jason L. Strickland ⁹, Mark J. Margres ^{1,*}

¹Department of Integrative Biology, University of South Florida, Tampa, FL, USA

²School of Biological Sciences, Washington State University, Pullman, WA, USA

³Biological Sciences Department, Clemson University, Clemson, SC, USA

⁴Facultad de Ciencias Biológicas, Universidad Juárez del Estado de Durango, Durango, Mexico

⁵Herp.MX®, Colima, Mexico

⁶Facultad de Ciencias Biológicas y Agropecuarias, Universidad Veracruzana, Veracruz, Mexico

⁷PIMVS Herpetario Palancoatl, Veracruz, Mexico

⁸Department of Plant and Wildlife Sciences, Brigham Young University, Provo, UT, USA

⁹Department of Biology, University of South Alabama, Mobile, AL, USA

*Corresponding authors: E-mails: hirsts@usf.edu; margres@usf.edu.

Accepted: September 02, 2024

Abstract

Understanding the proximate and ultimate causes of phenotypic variation is fundamental in evolutionary research, as such variation provides the substrate for selection to act upon. Although trait variation can arise due to selection, the importance of neutral processes is sometimes understudied. We presented the first reference-quality genome of the Red Diamond Rattlesnake (*Crotalus ruber*) and used range-wide ‘omic data to estimate the degree to which neutral and adaptive evolutionary processes shaped venom evolution. We characterized population structure and found substantial genetic differentiation across two populations, each with distinct demographic histories. We identified significant differentiation in venom expression across age classes with substantially reduced but discernible differentiation across populations. We then used conditional redundancy analysis to test whether venom expression variation was best predicted by neutral divergence patterns or geographically variable (a)biotic factors. Snake size was the most significant predictor of venom variation, with environment, prey availability, and neutral sequence variation also identified as significant factors, though to a lesser degree. By directly including neutrality in the model, our results confidently highlight the predominant, yet not singular, role of life history in shaping venom evolution.

Key words: transcriptomics, population genomics, ontogeny, venom.

Significance

Although the neutral theory of molecular evolution has provided a null model for >50 years when examining the genetics underlying phenotypes, neutral processes are not always explicitly incorporated into trait-based analyses. Snake venoms evolve quite rapidly and are often assumed to be evolving solely under strong directional selection. Here, we present the first reference-quality genome of the Red Diamond Rattlesnake and use range-wide 'omic data to estimate the degree to which neutral and adaptive evolutionary processes shape venom evolution. We found that life-history evolution was the dominant force underlying venom variation. Following life history, however, neutral sequence variation explained comparable variation to both biotic and abiotic factors, suggesting that neutral processes play a more prominent role than previously thought.

Introduction

Natural populations often exhibit exceptional degrees of phenotypic variation (Darwin 1859; Nevo 1978), such as body color of strawberry poison frogs (Summers et al. 2003; Yang et al. 2019), body and beak size of Galápagos Island finches (Darwin 1859; Grant and Grant 2002), and levels of salinity resistance in salt marsh plants (Hester et al. 2001) among others (Hoekstra et al. 2006; Dickson et al. 2017). Such variation can be the product of adaptive and/or neutral evolutionary processes (Lande 1976). Neutrality often serves as the evolutionary null hypothesis (Fisher 1930; Kimura 1968; Ohta 1973; Nei 2005; Müller et al. 2022), as it provides a baseline against which the effects of natural selection can be measured (Serra et al. 2013; Rohlf et al. 2014; Zhang 2018). Phenotypic variation, however, is frequently explored solely within the framework of selection and adaptation (Gould and Lewontin 1979; Brodie et al. 2002; Williams et al. 2003; Hanifin et al. 2008; Smith et al. 2023), even when such variation may be the product of neutral evolutionary processes via geographically limited dispersal and consequent gene flow (Lande 1976; Alexander et al. 2006). Indeed, a textbook example of phenotypic variation assumed to be adaptive is toxin production in rough-skinned newts (*Taricha granulosa*). Newt toxin production may be a response to coevolutionary interactions with a toxin-resistant predator, the common garter snake (*Thamnophis sirtalis*; Brodie and Brodie 1990; Brodie et al. 2002, 2005; Williams et al. 2003, 2010). Recently, a robust statistical framework accounting for demographic histories and population structure demonstrated that *T. granulosa* toxicity levels were more significantly predicted by population structure and isolation-by-distance (IBD) rather than resistance levels of *T. sirtalis* (Hague et al. 2020), indicating that neutral evolutionary processes were substantially contributing to variation in toxin production. The relationship between population structure and toxin production in *T. granulosa* highlights the importance of determining whether other traits assumed to be evolving under strong selection actually exhibit patterns consistent with *only* adaptive evolution (Zhang 2018).

Recently, snake venom has emerged as an effective system for studying adaptive evolution (Margres et al. 2017a; Arbuckle 2020; Mason et al. 2022; Rao et al. 2022). However, neutral evolution in this system is occasionally untested (Sanz et al. 2006; Barlow et al. 2009; Cipriani et al. 2017; Smiley-Walters et al. 2017; Davies and Arbuckle 2019; Smith et al. 2023) despite evidence that neutral processes, such as genetic drift, may play a role in shaping venom characteristics (Sasa 1999; Aird et al. 2017; Casewell et al. 2020; Rao et al. 2022). Snake venom is a complex, polygenic trait composed of 40–100 proteinaceous toxins used for prey immobilization, digestion, and defense (Daltry et al. 1996; Barlow et al. 2009; Casewell et al. 2011; Mackessy 2021). Despite the complex genomic architecture of venom (Schield et al. 2019; Margres et al. 2021a; Hogan et al. 2024), toxin gene expression is specific to venom glands (Rokyta et al. 2015), with differences in expression having clear, functional effects on the venom phenotype (Barlow et al. 2009; Holding et al. 2016; Margres et al. 2017a; Smiley-Walters et al. 2017; Casewell et al. 2020). Venom expression exhibits extensive variation across different species (Casewell et al. 2014; Margres et al. 2015a; Jackson and Fry 2016; Jackson et al. 2016; Durban et al. 2017; Pla et al. 2019; Senji Laxme et al. 2019; Holding et al. 2021), populations of the same species (Massey et al. 2012; Margres et al. 2015a, 2019; Holding et al. 2018; Smith et al. 2023), and life histories (Andrade and Abe 1999; Alape-Girón et al. 2008; Barlow et al. 2009; Margres et al. 2015a, 2015b; Wray et al. 2015; Modahl et al. 2016; Cipriani et al. 2017; Durban et al. 2017; Rokyta et al. 2017; Borja et al. 2018; Schonour et al. 2020); venom expression variation at all three scales has also been shown to be the result of genetic rather than environmental (i.e. plastic) effects (Gibbs et al. 2009; Margres et al. 2015b). Abiotic and/or biotic selective pressures, such as differences in environment (Strickland et al. 2018; Margres et al. 2021b; Siqueira-Silva et al. 2021), diet (Mackessy et al. 2003; Holding et al. 2018; Schonour et al. 2020; Holding et al. 2021), or prey venom resistance (Barlow et al. 2009; Holding et al. 2016; Margres et al. 2017a), may produce such variation.

Antagonistic coevolutionary interactions with prey have been associated with venom expression variation in certain cases (Barlow et al. 2009; Holding et al. 2016; Margres et al. 2017a); however, prey-driven selection is often assumed to produce venom expression variation without sufficient empirical evidence (e.g. Smith et al. 2023). Determining whether venom expression variation is adaptive requires both precise knowledge of diet and quantitative and functional measurements of venom effectiveness in multiple prey species and populations, making it exceptionally difficult to test (Barlow et al. 2009; Holding et al. 2016; Margres et al. 2017a; Smiley-Walters et al. 2017; Casewell et al. 2020). Consequently, venom studies often rely on methods for detecting signatures of selection such as *dN/dS* ratios (Juárez et al. 2008; Margres et al. 2013; Rokyta et al. 2013; Mason et al. 2020; Zhao et al. 2021), but changes to gene-expression patterns have, in general, been found to explain a disproportionate amount of venom expression variation (Margres et al. 2016a, 2017a, 2017b), consistent with other traits (Gompel et al. 2005; Fraser 2013; Konczal et al. 2015). Nevertheless, venom expression variation should not be exclusively attributed to adaptive evolution without investigating the potential role of neutral evolutionary processes (Sasa 1999; Casewell et al. 2020; Rao et al. 2022). Much like the variable toxin production observed across *T. granulosa* populations, geographic variation in snake venom expression may be erroneously attributed solely to selection, whereas it may arise, at least in part, from neutral evolutionary processes.

The Red Diamond Rattlesnake (*Crotalus ruber*) exhibits ontogenetic and geographic venom variation (Straight et al. 1992), making it an excellent focal species for investigating the contributions of neutral and adaptive processes on snake venom evolution. *Crotalus ruber* is a large-bodied pitviper found in western North America ranging from San Bernadino County, California, USA, south throughout the Baja California peninsula and various islands. Habitat throughout its range varies extensively (Grismer 2002), and its prey composition, which includes primarily small- to medium-sized mammals, is well characterized (Dugan and Hayes 2012). Two mainland subspecies are recognized: *C. r. ruber* extends from the northern range edge to the central region of the Baja peninsula, and *C. r. lucasensis* inhabits the southern third of the Baja peninsula (Fig. 1). The current subspecies definitions are based on morphological (Grismer 2002) and genetic differentiation, with divergence occurring ~570 ka before present (Harrington et al. 2018). Although *C. ruber* exhibits venom variation in specific protein families across its geographic range and life history (Straight et al. 1992; Pozas-Ocampo et al. 2020), variation across the complete venom phenotype as well as the evolutionary processes producing such variation have yet to be investigated.

In this study, we investigated the evolutionary processes, both adaptive and nonadaptive, that may have produced

variation in a trait that is often assumed to be evolving under strong directional selection. We aimed to 1) generate the first reference *C. ruber* genome for use in downstream analyses, 2) characterize neutral population structure and demographic history, 3) quantify venom expression variation across populations and life-history stages, and 4) determine the relative contributions of neutral evolutionary processes, geographically variable abiotic and/or biotic factors, and life history in explaining venom expression evolution through robust statistical models. If venom is rapidly evolving due to selection, we expect decoupling of patterns produced by neutral evolutionary processes, such as population structure and IBD (Wright 1943; Williams et al. 1988; Keller et al. 2009), with venom variation spatially, as demonstrated previously (Margres et al. 2019). Specifically, we would expect patterns of venom variation to correlate with patterns of variation in abiotic and/or biotic factors such as dietary composition or climate (Holding et al. 2018). Conversely, if venom is evolving due to neutral processes, we expect a strong correlation between neutral sequence variation and venom variation, similar to what was found for toxin-production levels in newts (Hague et al. 2020). Overall, our approach integrating diverse data types from multiple individuals across the range will allow us to identify the most significant factors driving venom evolution within a species.

Materials and Methods

Sampling

We collected 21 *C. ruber* across the Baja California Peninsula, MX and southern California, USA (Fig. 1). Snakes were captured via road cruising or visual encounter surveys. Upon capture, sampling locality, snout–vent–length (SVL), tail length, and sex were recorded. Venom and blood were sampled in the field from two individuals prior to release. Nineteen individuals were euthanized, dissected, vouchered, and deposited at La Colección Herpetologica de la Facultad de Ciencias Biológicas de la Universidad Juárez del Estado de Durango in Gómez Palacio, Durango, MX. For dissection, we removed the right and left venom glands, heart, liver, gonad, kidney, muscle, and/or blood and stored each tissue in RNALater and/or 95% ethanol. Snakes were collected under the following permits: Secretaría de Medio Ambiente y Recursos Naturales Oficio N SGPA/DGVS/01090/17; SGPA/DGVS/002288/18; SGPA/DGVS/13338/19; SGPA/DGVS/2190/19; SGPA/DGVS/08831/20; SGPA/DGVS/10362/21 and California Department of Fish and Wildlife SC-12985. The procedures outlined were approved by the University of South Florida Institutional Animal Care and Use Committee (IACUC) under protocol IS00011949 and Clemson University IACUC protocol 2017-067.

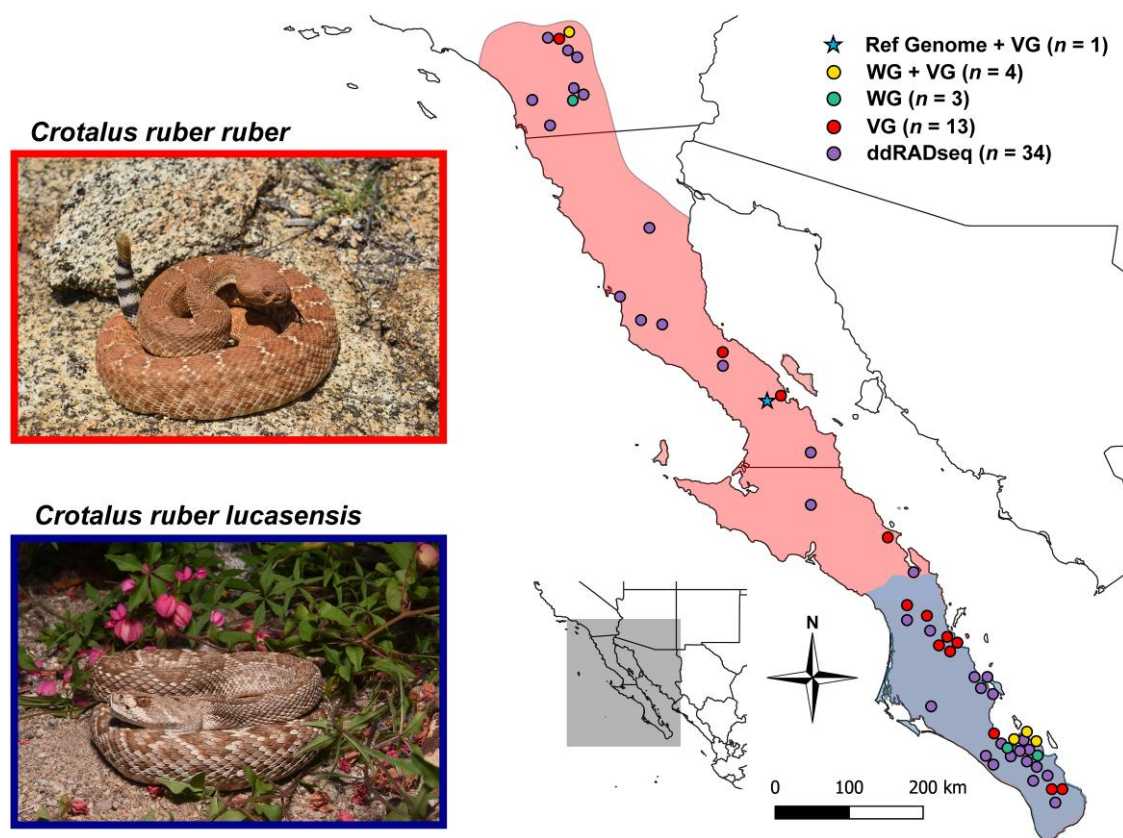


Fig. 1. Distribution and sampling map of *Crotalus r. ruber* (red map shading) and *C. r. lucasensis* (blue map shading). Color of sampling point is based on the types of data generated for the individual sampled at that location. Ref Genome, PacBio HiFi genome sequencing; WG, short-read whole-genome sequencing; VG, venom-gland transcriptomes; ddRADseq, double digest restriction-site associated DNA Sequencing. Snake image credits: Ricardo Ramírez Chaparro.

Reference Genome Sequencing and Assembly

A high-quality reference genome for *C. ruber* was produced from a subadult male (66.5 cm SVL, 71.0 cm TL) sampled near Bahía de los Ángeles, Baja California, MX (Fig. 1). High-molecular-weight (HMW) genomic DNA (gDNA) was obtained from blood extracted from the caudal vein. The genome was sequenced using Pacific Biosciences HiFi sequencing on 1.5 cells on the Sequel II sequencer at the University of Delaware Sequencing & Genotyping Center. We used HiFiAdapterFilt (Sim et al. 2022) to detect adapter contamination in the sequenced reads and found 1,259 reads (0.00094% of total) with adapters. We assembled the genome using all reads with the Hifiasm assembler (Cheng et al. 2021). We then used Blast (Johnson et al. 2008) with the UniVec database to detect adapters within the assembly and masked all adapter contaminants using the BEDTools maskfasta function (Dale et al. 2011). Assembly quality statistics were calculated using MERQURY (Rhie et al. 2020) and Genome Tools (Gremme et al. 2013). Assembly completeness was assessed using BUSCO (Simão et al. 2015) for datasets Vertebrata and Sauropsida. We screened for foreign contamination of

the assembled genome using NCBI FCS-GX (Astashyn et al. 2024; Bush et al. 2024; Pozo et al. 2024). No contamination was detected in the genome assembly and classification of all contigs was consistent with the expected taxonomic composition of the target organism. To achieve a chromosomal representation of the assembly, we aligned the *C. ruber* genome to the *Crotalus adamanteus* genome (Hogan et al. 2024) using Ragtag (Alonge et al. 2022). A Circos plot of the genome was generated using the Circlize package (Gu et al. 2014) in R. Genome assembly and all data generated in this study are available at NCBI PRJNA1051499.

Reference Genome Annotation

To aid in genome annotation, we generated transcriptomes for blood, gonad, heart, kidney, liver, and right and left venom glands from the same subadult male used for reference genome assembly (see below for details on RNA extraction and sequencing); all RNA-seq data were aligned to the genome using Hisat2 (Kim et al. 2019). The genome was then annotated using GeMoMa (Keilwagen et al. 2019) with the *Crotalus adamanteus* (Hogan et al. 2024)

genome and the aligned *C. ruber* transcriptome data as references. Functional annotations were added using InterProScan (Jones et al. 2014) and Blast (Johnson et al. 2008). Due to the complex architecture of venom genes in large-tandem arrays, automated annotation of venom genes is often unreliable. As such, we used Geneious Prime (Kearse et al. 2012) and FGENESH+ (Salamov and Solovyev 2000) to manually identify and annotate venom genes as previously described (Margres et al. 2021a).

ddRADseq Data Processing

We downloaded double digest restriction-site associated DNA (ddRADseq) data for 34 *C. ruber* from NCBI SRA (Fig. 1; PRJNA413434; Harrington et al. 2018). Nonreference based population genomic analyses can be prone to errors arising from repetitive regions, polymorphisms, and sequencing errors (Brandies et al. 2019); therefore, we reanalyzed the *C. ruber* ddRADseq data using reference-based alignment to the generated reference genome described above. All ddRADseq data were aligned to the reference genome using iPyrAD (Eaton and Overcast 2020) using default parameters.

Whole-Genome Sequencing Data Generation and Processing

We generated short-read whole-genome sequencing (WGS) data for six *C. ruber* (PRJNA1051499) and downloaded an additional *C. ruber* whole-genome from NCBI SRA (PRJNA593834; Schield et al. 2022). For the six genomes generated in this study, DNA was isolated from blood samples using the EZNA Tissue DNA Kit (Omega Bio-tek), and DNA libraries were generated using the Ultra II FS DNA Library Prep kit (New England Biolabs). Libraries were sequenced at the North Carolina State University Genomic Sciences Laboratory using Illumina Novaseq 6,000 with 150 paired-end sequencing (supplementary table S6, Supplementary Material online). Data were mapped to the reference genome using bowtie2 (Langmead and Salzberg 2012), and SNPs were called using GATK (McKenna et al. 2010) best practices workflow for germline short variant discovery with default parameters and recommended hard filters. A merged VCF file with the 34 ddRADseq samples and seven WGS samples was produced using bcftools merge and was subsequently filtered using VCFtools (Danecek et al. 2011) with the following parameters: minimum allele frequency (maf) 0.05, minimum depth (minDP) 5, and max-missing 0.5. The final combined genomic dataset included 41 individuals and 5,284 SNPs.

Transcriptome Sequencing

We sequenced venom-gland transcriptomes from 12 individuals and additional blood, gonad, heart, kidney,

and liver transcriptomes for the reference genome animal (PRJNA1051499) as outlined above. We also downloaded six additional venom-gland transcriptomes from NCBI SRA (PRJNA88989; Holding et al. 2021). Venom glands were processed following the approach of Rokyta et al. (2012). Briefly, for venom glands, venom was extracted four days prior to euthanasia to allow maximum transcription upon venom gland extraction (Rotenberg et al. 1971). At four days, snakes were euthanized and dissected. For dissection, the left and right venom glands, heart, blood, muscle, kidney, liver, and gonad were removed and placed in RNALater. We extracted RNA from the left and right venom glands separately, then combined in equal quantities for RNA library prep for each snake. For the reference genome snake, we also extracted RNA from each of the tissues listed above. We isolated RNA using a TRIzol extraction method as outlined in Rokyta et al. (2017). RNA libraries were generated using the Ultra II RNA Library Prep Kit for Illumina (New England Biolabs) and sequenced at the Florida State University DNA Sequencing Facility using NovaSeq 6,000 and the Oklahoma Medical Research Foundation Clinical Genomics Center using the NovaSeq X Plus with 150 paired-end sequencing (supplementary table S6, Supplementary Material online). Because gene expression values are sensitive to the read count methods employed, particularly for genes with exceptionally low and high expression (Liu et al. 2022), we mapped each transcriptome to the generated reference genome using Hisat2 (Kim et al. 2019) and estimated read counts for genes using both HTSeq-count (Anders et al. 2015; Putri et al. 2022) and Stringtie2 (Pertea et al. 2015). We used these two read-count estimation methods to provide complementary yet distinct quantitative estimates of gene expression to account for potential biases inherent in each approach. StringTie2 assembles RNA transcripts and estimates gene expression based on these assembled transcripts. HTSeq-counts directly counts the number of reads mapped to predefined features (e.g. genes labeled in a GFF3 annotation file), providing a direct measure of gene expression but potentially overlooking transcript complexity, such as alternative splicing or multiple isoforms, which may be better accounted for by StringTie2.

Estimating Population Structure and Neutral Genetic Divergence

To recharacterize *C. ruber* population structure (Harrington et al. 2018), we used conStruct (Bradburd et al. 2018) on the combined genomic dataset ($n = 41$) described above. We removed SNPs with >30% missing data and subsequently removed two individuals with >50% missing data for a reduced dataset containing 39 individuals and 2,241 SNPs. We initially tested $K = 1-5$ genetic clusters using both spatial and nonspatial models and compared

predictive accuracies using cross-validation. For each value of K and each type of model, we ran cross-validation using 20 replicates and 10,000 iterations, with SNPs split into 75% training and 25% testing data partitions. We ran each model for 20,000 iterations using three independent MCMC replicates. Additionally, we investigated patterns of sequence dissimilarity across all individuals and SNPs ($n = 41$; 5,284 SNPs) using principal coordinate analysis (PCoA) from the R package *dartR* (Gruber et al. 2018). We then calculated F_{ST} between the defined populations using *VCftools* (Danecek et al. 2011) on both the full ($n = 41$; 5,284 SNPs) and reduced ($n = 39$; 2,241 SNPs) genomic dataset.

Estimating Effective Migration Surfaces

To infer migration rates in *C. ruber*, we used EEMS (Petkova et al. 2016) on the full combined genomic dataset ($n = 41$; 5,284 SNPs). We converted the merged WGS and ddRADseq SNP dataset to PLINK format (Purcell et al. 2007) and transformed the data to a pairwise distance matrix using “bed2diffs” function in EEMS. We used EEMS to estimate migration surfaces by running three independent chains, each with 1,000 demes, 10,000,000 MCMC iterations, 1,000,000 iterations of burn-in, and a thinning interval of 10,000. All chains successfully converged (supplementary fig. S5, Supplementary Material online).

Estimating Demographic History

To estimate effective population size (N_e) through time for each *C. ruber* population as identified in *conStruct* above, we used pairwise sequentially Markovian coalescence (PSMC; Li and Durbin 2011). We used PSMC over similar methods (e.g. MSMC, SMC++, Stairway Plot; Schiffels and Durbin 2014; Liu and Fu 2015; Terhorst et al. 2017) due to its higher precision and accuracy, especially during intermediate ($\sim 10,000$ – 666 generations) time periods (Patton et al. 2019); however, PSMC may imprecisely estimate (N_e) towards the present (Liu and Fu 2015; Nadachowska-Brzyska et al. 2016; Patton et al. 2019). Therefore, interpretations of historical demographic history based on our analyses were limited to intermediate evolutionary timescales as defined above. We inferred N_e across 28 free atomic time intervals ($4+25*2+4+6$) and checked for variance in N_e estimation by performing 100 bootstrap replicates (supplementary fig. S6, Supplementary Material online). We used the published generation time ($g = 3.3$) and mutation rate ($\mu = 0.7 \times 10^{-8}$) of sister taxon *Crotalus atrox* (Castoe et al. 2007; Holding et al. 2021).

Venom Proteomics

To characterize *C. ruber* venom variation, we collected venom from 20 individuals and used reversed-phase high performance liquid chromatography (RP-HPLC) to quantify

venom protein expression. Venom was collected and then dried and stored at -80°C prior to analysis. We conducted RP-HPLC on a Dionex ultimate 3000 UHPLC DAD (Thermo Fisher Scientific) and a BeckmanSystem Gold HPLC (BeckmanCoulter) using a Jupiter $5\mu\text{m}$ C18 300 Å, LC Column 250 *times* 2 mm, Ea column. $50\mu\text{g}$ of total venom protein were injected onto the column using a solvent system of A = 0.1% trifluoroacetic acid (TFA) in water and B = 0.075% TFA in acetonitrile. After five minutes at 5% B, a 1% per minute linear gradient of A and B was run to 25% B, followed by a 0.25% per minute gradient from 25% to 65% B at a flow rate of 0.6 mL per min (Margres et al. 2014). Column effluent was monitored at 220 nm. RP-HPLC peaks were quantified in the Chromeleon software (Thermo Fisher Scientific). To estimate the relative abundance of each protein peak, we measured the area under the peak relative to the total area of all peaks identified (Gibbs and Rossiter 2008). Prior to statistical analyses, quantified peaks were transformed in R using isometric Log-Ratio (ILR) from the *rombCompositions* package (Templ et al. 2023).

Characterizing Venom Expression Differentiation

To identify patterns of venom expression variation, we first conducted a PCA on the ILR transformed venom proteomic data ($n = 20$) in R using the “prcomp” function from the *Stats* package. We then conducted a simple regression model (“lm” function in R) comparing PC1 with SVL to test for the effects of ontogeny, which is common in rattlesnakes (Andrade and Abe 1999; Alape-Girón et al. 2008; Barlow et al. 2009; Margres et al. 2015a, 2015b; Wray et al. 2015; Modahl et al. 2016; Cipriani et al. 2017; Durban et al. 2017; Rokyta et al. 2017; Borja et al. 2018; Schonour et al. 2020). To determine whether venom protein expression was significantly different across populations and/or age classes, we performed a permutational multivariate analysis of variance (PERMANOVA) in the “adonis2” function of the *vegan* package (Oksanen et al. 2020) on the ILR transformed venom proteomic data. The same approach using PCA, simple regression, and PERMANOVA was repeated using normalized venom-gland transcriptomic data from HTSeq-count ($n = 18$; Anders et al. 2015; Putri et al. 2022) to verify concordance between venom proteomic and venom-gland transcriptomic data. Read count data from HTSeq-count were normalized using median of ratios from DESeq2 (Anders and Huber 2010).

We also tested whether specific toxin transcripts were significantly differentially expressed (DE) across populations and/or age classes using the program DESeq2 (Love et al. 2014) on our venom-gland transcriptome data ($n = 18$). For the geographic comparison, we used the two populations as delineated from *conStruct* (Bradburd et al. 2018) and accounted for ontogeny in the model by using age class

as a covariate. For the ontogenetic comparison, we accounted for geography in the model by including population as a covariate. Significance in differential expression was calculated using the FDR-adjusted P value (P_{adj}) and \log_2 fold change (LFC) ≥ 1 from DESeq2.

Determining the Contributions of Ecological and Evolutionary Factors on Venom Expression Variation through Conditional Redundancy Analysis

To estimate the contributions of neutral processes, life history (i.e. snake size), prey availability and diversity, and climactic conditions on *C. ruber* venom expression variation, we used conditional Redundancy Analyses (RDA; van den Wollenberg 1977; Liu 1997; Capblancq and Forester 2021). Briefly, conditional RDA controls for the effects of one set of explanatory variables prior to conducting RDA on the residual matrix. RDA functions as an extension to multiple regression analysis but permits multivariate response variables. Significance testing within an RDA framework utilizes permutation, making it robust to small sample size and distributional assumptions (Liu 1997).

Here, we explored venom expression variation using eight different response variables: (i) estimated read counts for all toxin genes using HTSeq-counts (Anders et al. 2015; Putri et al. 2022), (ii) estimated read counts for all toxin genes using Stringtie2 (Pertea et al. 2015) and (iii–viii) estimated read counts for specific paralogs belonging to the six dominant toxin families individually using HTSeq-counts. All venom response variables were multivariate toxin gene expression data representing the abundance levels of multiple toxin loci, enabling us to identify the most significant explanatory variables influencing the expression of toxin genes within a multivariate framework. Prior to analyses, we transformed read count data using the median of ratios in DESeq2 (Anders and Huber 2010). We conditioned each explanatory variable (nontoxin sequence variation, toxin sequence variation, climactic variation, prey availability, and prey diversity, each described below) in the model on the other explanatory variables to remove the potential confounding effects for each. We then conducted a marginal test using all explanatory variables and used forward model selection to generate the marginal model (i.e. best model). Conditional RDAs were conducted using the “*rda*” function from the Vegan package in R (Oksanen et al. 2020) and included the “*anova*” function for significance testing, “*RsquareAdj*” for model fit, and “*ordiR2step*” for forward model selection. We describe each explanatory variable below:

1. To include the contributions of neutral processes in the model, we generated a SNP dataset for nontoxin genes, our proxy for neutrality (Rautsaw et al. 2019; Holding et al. 2021), sequenced from the venom-gland transcriptomes ($n = 18$). We used GATK (McKenna et al. 2010) with default parameters as previously outlined. Additional filtering parameters from VCFtools (Danecek et al. 2011) included min-alleles 2, minDP 5, max-missing 0.5, and minimum allele frequency of 0.1. We converted our annotated reference genome file to a BED file and used VCFtools with functions “*bed*” and “*exclude-bed*” to isolate nontoxin genes from toxin genes, resulting in 41,236 nontoxin SNPs for analysis. We also attempted to remove potential signatures of selection from the nontoxin SNP data by creating a second dataset containing only synonymous sites. Variant annotation was conducted using SnpEff (Cingolani et al. 2012), resulting in 3,818 nontoxin synonymous SNPs. Nontoxin sequence variation was summarized using principal Coordinate Analysis (PCoA) from the R package dartR (Gruber et al. 2018) on both the full nontoxin SNP dataset (41,236 SNPs) and the nontoxin synonymous SNP dataset (3,818 SNPs; [supplementary fig. S2B-C, Supplementary Material online](#)). To determine whether the inclusion of other nontoxin SNP types (nonsynonymous and intronic) accurately represented neutral genetic divergence, we conducted a regression using PCo1 of the full nontoxin SNP dataset and PCo1 of the nontoxin synonymous SNP dataset ([supplementary fig. S4, Supplementary Material online](#)). We retained PCo1 and PCo2 of the full nontoxin SNP dataset (41,236 SNPs) for use in the conditional RDAs ([supplementary table S7, Supplementary Material online](#)).
2. To include signatures of selection on toxin gene sequences, we summarized toxin sequence variation from venom-gland transcriptomes ($n = 18$) following the same approach above; however, following filtration, toxin genes were isolated from nontoxin genes, resulting in a toxin-only SNP dataset of 1,760 SNPs. Note that toxin sequence variation was excluded as a variable in individual toxin families due to the limited number of independent SNPs for each family ([supplementary fig. S2D and table S7, Supplementary Material online](#)).
3. Abiotic factors were incorporated using differing environmental conditions as represented by the 19 Worldclim Bioclim variables (Hijmans et al. 2005) at each sampling site using 5 min spatial resolution. We conducted a PCA across the data, and PC1 and PC2 were retained for use in the conditional RDAs (See [supplementary table S4, Supplementary Material online](#) for PC loadings and proportion of variance explained by each PC).
4. To account for potential differences in diet between individuals, we incorporated prey availability in the model following the approach of Holding et al. (2018). Prey availability was determined using published accounts of prey data for *C. ruber* (Klauber 1997; Clark et al.

2012; Dugan and Hayes 2012; Holding et al. 2021) resulting in 29 known prey items (supplementary table S5, Supplementary Material online). Geographic range was determined for each prey item using iNaturalist (www.inaturalist.org), IUCN (www.iucn.org), and/or Map of Life (mol.org). For each sample site, each prey item was given a value of “1” if present and “0” if absent (supplementary table S7, Supplementary Material online). We conducted Nonmetric multidimensional scaling (NMDS) on the prey dataset using the “metaMDS” function from the Vegan package in R (Oksanen et al. 2020) and retained MDS1 and MDS2 for use in the conditional RDAs (See supplementary table S5, Supplementary Material online for NMDS loadings and proportion of variance explained by each MDS).

- Phylogenetic diversity of prey has been shown to predict patterns of venom evolution across species (Holding et al. 2021); therefore, we incorporated estimates of prey mean phylogenetic distance (MPD) in the model. We generated a phylogeny of the 29 *C. ruber* prey items using www.timetree.org (supplementary fig. S7, Supplementary Material online; Kumar et al. 2017) and used the “ses.mpd” function from the Picante R package (Kembel et al. 2010) to calculate MPD at each site (supplementary table S8, Supplementary Material online).

See supplementary table S7, Supplementary Material online for data used in conditional RDAs.

Results

De Novo Genome Assembly and Annotation

We generated a reference *C. ruber* genome using PacBio HiFi reads (~20× coverage) for a subadult male collected within the *C. r. ruber* range near Bahía de los Ángeles, Baja California, MX (Fig. 1). Genome assembly length was 1.59 Gb (1,126 contigs, N50 of 6.25 Mb, L50 of 65; Table 1). We calculated additional genome quality assessment metrics, such as phred quality score (55), k-mer completeness (96%), and BUSCO (96.5% complete Vertebrata; 93.0% complete Sauropsida; Table 1). To achieve a chromosome-level assembly, we scaffolded the *C. ruber* assembly to the chromosome-level assembly of the Eastern Diamondback Rattlesnake (*C. adamanteus*; Hogan et al. 2024) using RagTag (Alonge et al. 2022). The number of contigs in the assembly was reduced ~10× to 111 scaffolds (N50 of 206.58 Mb), and all 17 autosomes assembled for *C. adamanteus* were assembled for *C. ruber*. Because our genome individual was male, only the Z sex chromosome was assembled (Fig. 2a). We annotated the genome and identified 20,771 protein-coding genes including 94 putative toxin genes within 14 toxin families (Fig. 2a). Multiple toxin families were found on microchromosomes

Table 1 Genome assembly statistics for *C. ruber*

Metric	
Assembly size (Gb)	1.59
Number of contigs	1,126
Contig N50 (Mb)	6.25
Contig L50	65
Number of scaffolds	111
Scaffold N50 (Mb)	206.58
bp anchored to chromosomes (Gb)	1.57 (98.7%)
Phred quality score (Q)	55
k-mer completeness %	96
BUSCO Vertebrata (C—D—F—M) %	96.5 — 1.0 — 1.1 — 2.4
BUSCO Sauropsida (C—D—F—M) %	93.0 — 1.2 — 1.2 — 5.8
CG content, %	39.8
Repeat content, %	49.07
Protein-coding genes	20,771
Putative venom protein-coding genes	94

All metrics are for the *de novo* assembly except “Number of scaffolds”, “Scaffold N50”, and “bp anchored to chromosomes” which represent metrics for the RagTag assembly to *C. adamanteus*. BUSCO metrics are shown as complete (C), duplicated (D), fragmented (F), and missing (M). Genome assembly available at NCBI PRJNA1051499.

(chromosomes 9–18 in Fig. 2a) as large tandem arrays, consistent with toxin genomic organization in other rattlesnakes (Schield et al. 2019; Margres et al. 2021a; Hogan et al. 2024).

Population Genomics Identifies Distinct Populations and Evolutionary Histories

We used conStruct (Bradburd et al. 2018) across 39 individuals (2,241 SNPs) to characterize population structure (Fig. 2b–c). Spatial models invariably had higher predictive accuracy than nonspatial models, with predictive accuracy reaching an asymptote at $K=2-3$ genetic clusters (supplementary fig. S1, Supplementary Material online). For the spatial models, additional genetic clusters beyond $K=2$ explained <5% of total genetic covariance, suggesting that $K=2$ was an appropriate choice for characterizing population genetic structure (Fig. 2b). After cross-validation, we fit final spatial models using the full dataset for $K=2$ and $K=3$. For $K=2$, populations were spatially sorted by latitude (Fig. 2b), with contact at ~26°N latitude, relatively consistent with current *C. ruber* subspecies delineation (Fig. 1; Grismer 2002). A similar pattern was observed for $K=3$ (Fig. 2c), with additional weak population structure at the northern range edge. We calculated the fixation index (F_{ST}) between the populations for $K=2$ in conStruct (hereinafter referred to as the north and south populations) using the full genomic dataset (north $n=19$; south $n=22$; 5,284 SNPs) as well as the reduced genomic dataset (north $n=18$; south $n=21$; 2,241 SNPs) used specifically for conStruct. We found that $F_{ST}=0.295$ and 0.301 , respectively. We also visualized patterns of sequence dissimilarity using the full genomic dataset

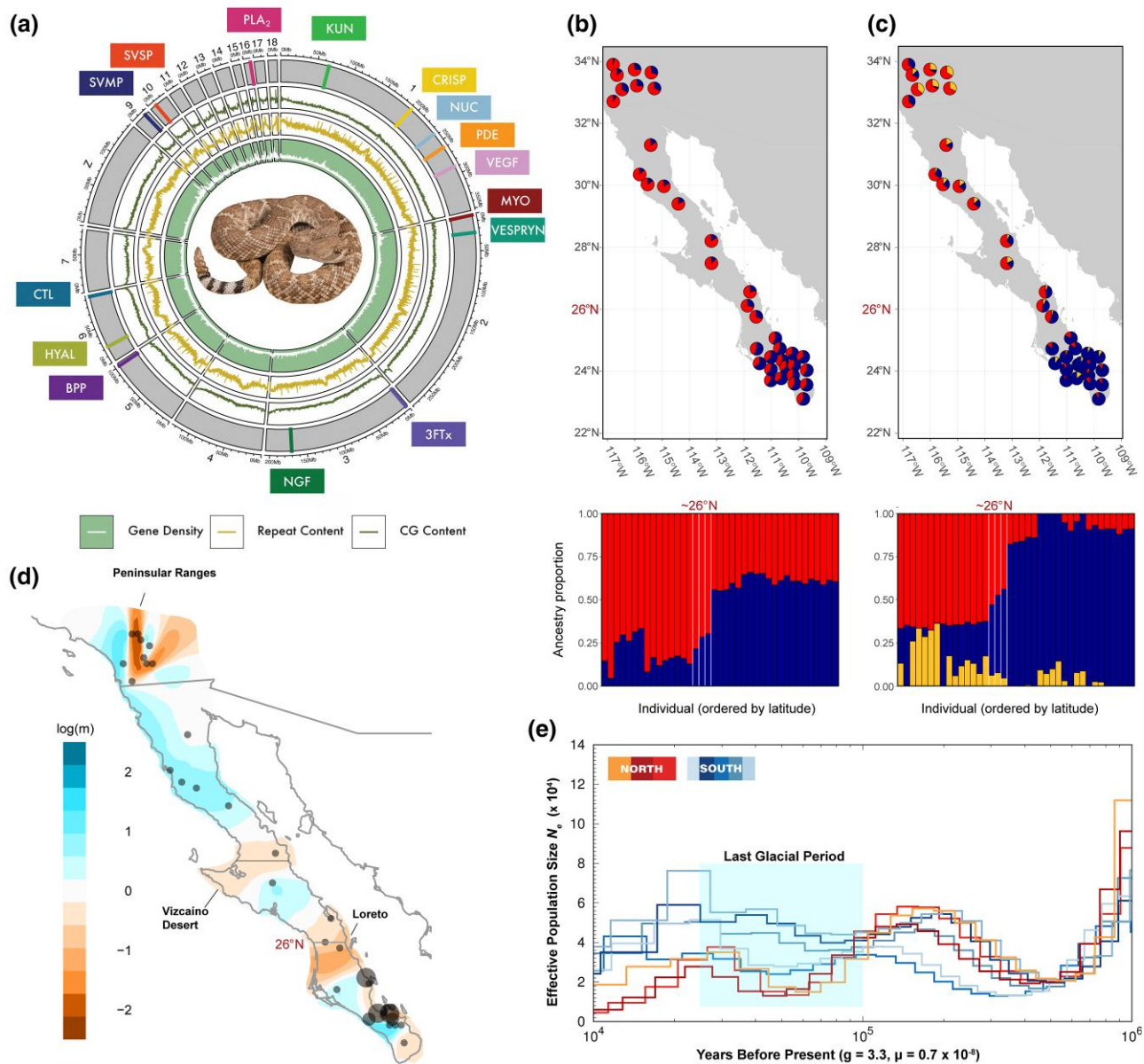


Fig. 2. Reference genome assembly and genomic sequencing of *C. ruber* reveals two genetically distinct populations with unique demographic histories. a) Circos plot of the RagTag reference genome assembly displaying gene density, repeat content, CG content, and toxin gene families mapped to chromosome scaffolds as represented by corresponding colored lines. Toxin families are (ordered by chromosome): KUN, Kunitz-type toxin; CRISP, cytesine-rich secretory protein; NUC, nucleotidase; PDE, phosphodiesterase; VEGF, vascular endothelial growth factor; MYO, myotoxin; 3FTx, three-finger toxin; NGF, nerve growth factor; BPP, bradykinin-potentiating peptide; HYAL, hyaluronidase; CTL, C-type lectin; SVMP, snake venom metalloproteinase; SVSP, snake venom serine proteinase; PLA₂, phospholipase A₂. b–c) Population structure characterized from short-read WGS and ddRADseq data using ConStruct spatial models with b) $K = 2$ and c) $K = 3$. Maps depict individuals as pie charts reflecting ancestry proportions contributed by each genetic cluster. d) Estimated effective migration surface from WGS and ddRADseq data using EEMS. Shading indicates areas with relatively high (orange) and low (blue) landscape resistance to gene flow compared to a null area-wide model of isolation-by-distance (IBD). Plotted values of $\log(m)$ are effective migration rates relative to the overall migration rate across the study area. Circles represent sampling locations, and circle size corresponds to sampling density. e) Estimates of demographic histories across the two distinct populations from panel (b). Lines represent effective population size (N_e) estimated from eight individuals using a generation length of 3.3 years and a mutation rate of 0.007 per lineage per million years. Colors indicate N_e estimates of individuals sampled from the northern population (warm) and southern population (cool; as determined in panel (b)). Contact zone ($\sim 26^\circ\text{N}$) is indicated throughout.

($n = 41$; 5,284 SNPs) using PCoA. Individuals clustered according to the population structure identified in conStruct; southern individuals clustered tightly along both PCo1 and

PCo2 while northern individuals clustered tightly along PCo1, but with increased variance along PCo2 (supplementary fig. S2A, Supplementary Material online).

Next, we estimated effective migration surfaces (EEMS; Petkova et al. 2016) using the full genomic dataset ($n = 41$; 5,284 SNPs) to explore spatially variable migration rates across the landscape and visualize departures from IBD (Fig. 2d). We observed three areas of relative reductions in gene flow: (i) the Peninsular Ranges of Southern California, (ii) the Vizcaíno Desert of the Baja Peninsula, and (iii) the current *C. ruber* subspecies boundary at $\sim 26^\circ\text{N}$ latitude near the town of Loreto, BCS, MX (Fig. 2d).

Lastly, we estimated demographic histories for the north ($n = 3$) and south ($n = 5$) populations using the Pairwise Sequentially Markovian Coalescent model (PSMC; Fig. 2e; Li and Durbin 2011) on our whole-genome data. Effective population size (N_e) decreased in both populations between ~ 100 and 200 ka before present and continued to decrease during the last glacial period (Broecker and Hemming 2001) between ~ 50 and 100 ka for the northern population while stabilizing in the southern population (Fig. 2e).

Venom Expression Varies Extensively Across Life History and Less So Across Geographic Space

We conducted a PCA on the venom proteomic data for 20 individuals (supplementary table S1, Supplementary Material online) and found that PC1 (65%) was primarily associated with SVL, with individuals clustering into two groups separated at ~ 65 cm SVL (supplementary fig. S3, Supplementary Material online). Indeed, a linear regression showed that venom PC1 was significantly correlated with SVL ($P < 0.001$, $\text{adj-}R^2 = 0.82$; supplementary fig. S3B, Supplementary Material online). To test for venom protein expression differentiation across age class (≤ 65 cm juvenile) and population (northern and southern populations as defined in conStruct), we conducted a PERMANOVA. Only ontogeny was significant ($P < 0.001$, $R^2 = 0.65$; adult $n = 14$; juvenile $n = 6$); neither population ($P = 0.194$, $R^2 = 0.03$; north $n = 11$; south $n = 9$) nor the interaction between age and population ($P = 0.275$, $R^2 = 0.02$) were significant. Overall, our proteomic analyses revealed that, at the trait level, venom expression was significantly different between age classes but not significantly different between populations.

To identify the specific toxin genes underlying ontogenetic venom variation and determine whether any individual toxin genes were significantly DE between populations, we generated venom-gland transcriptome data for 18 individuals across the range (Fig. 3). We first verified that the venom gland transcriptomic data exhibited similar patterns to those observed in the venom proteomic data by reconducting both PCA and PERMANOVA (Fig. 3a,b). PC1 (31%) was again significantly and positively correlated with SVL ($P < 0.001$, $\text{adj-}R^2 = 0.65$; Fig. 3a), and only ontogeny was significant in the PERMANOVA ($P = 0.005$, $R^2 = 0.31$;

adult $n = 13$; juvenile $n = 5$); neither population ($P = 0.200$, $R^2 = 0.07$; north $n = 12$; south $n = 6$) nor the interaction between age and population ($P = 0.590$, $R^2 = 0.02$) were significant.

We identified specific genes that were significantly DE across populations (Fig. 3c) and age classes (Fig. 3d). Between populations (north $n = 12$; south $n = 6$), four toxin genes were significantly DE, with all four genes (*C-type lectin [CTL]-1*, *CTL-2*, *snake venom metalloproteinase [SVMP]-mad-6*, *SVMP-mpo-1*) exhibiting higher expression in the northern population. Between age classes (adult $n = 13$; juvenile $n = 5$), while accounting for population, 27 toxin genes were significantly DE. The majority ($n = 21$) of the genes were biased toward adults (i.e. more highly expressed in adults than juveniles), with most genes belonging to the *SVMP* ($n = 9$) and *CTL* ($n = 6$) toxin families. Most juvenile-biased toxin genes ($n = 6$) belonged to the myotoxin gene family ($n = 3$). See supplementary table S2, Supplementary Material online for details of all DE transcripts between age groups and populations.

Conditional Redundancy Analysis Identifies Life History as the Most Predominant Driver of Venom Evolution

To determine the relative roles of putatively neutral and adaptive evolutionary processes in driving venom expression evolution, we used conditional RDA to estimate the effects of nontoxin sequence variation (our proxy for neutrality; supplementary fig. S2A-C, S4, Supplementary Material online), toxin sequence variation, abiotic environmental factors, and prey data (availability and phylogenetic distance) on multivariate venom expression data.

First, we used PCoA to determine whether (i) nontoxin SNPs accurately reflected patterns of neutral genomic sequence variation and (ii) patterns of nontoxin sequence variation were robust to the inclusion of nonsynonymous variants. Patterns of sequence variation under PCoA were consistent among neutral genomic SNPs, nontoxin synonymous SNPs, and nontoxin SNPs including all variant types (supplementary fig. S2, Supplementary Material online). Additionally, correlation between PCo1 of nontoxin synonymous SNPs and PCo1 of all nontoxin SNPs was highly significant (supplementary fig. S4, Supplementary Material online; $P < 0.001$; $R^2 = 0.97$). Therefore, nontoxin SNPs including all variant types served as a valid proxy for neutral patterns of genetic divergence.

Using conditional RDA with toxin gene read count estimations from HTSEQ-count as the multivariate response variable, the full model, including all variables, was significant ($P = 0.002$; $\text{adj-}R^2 = 0.73$; Table 2), indicating that our model captured at least one or more variables that significantly explained venom expression variation. The marginal (i.e. best) model ($\text{adj-}R^2 = 0.54$) as determined from forward model selection revealed that SVL ($P = 0.003$;

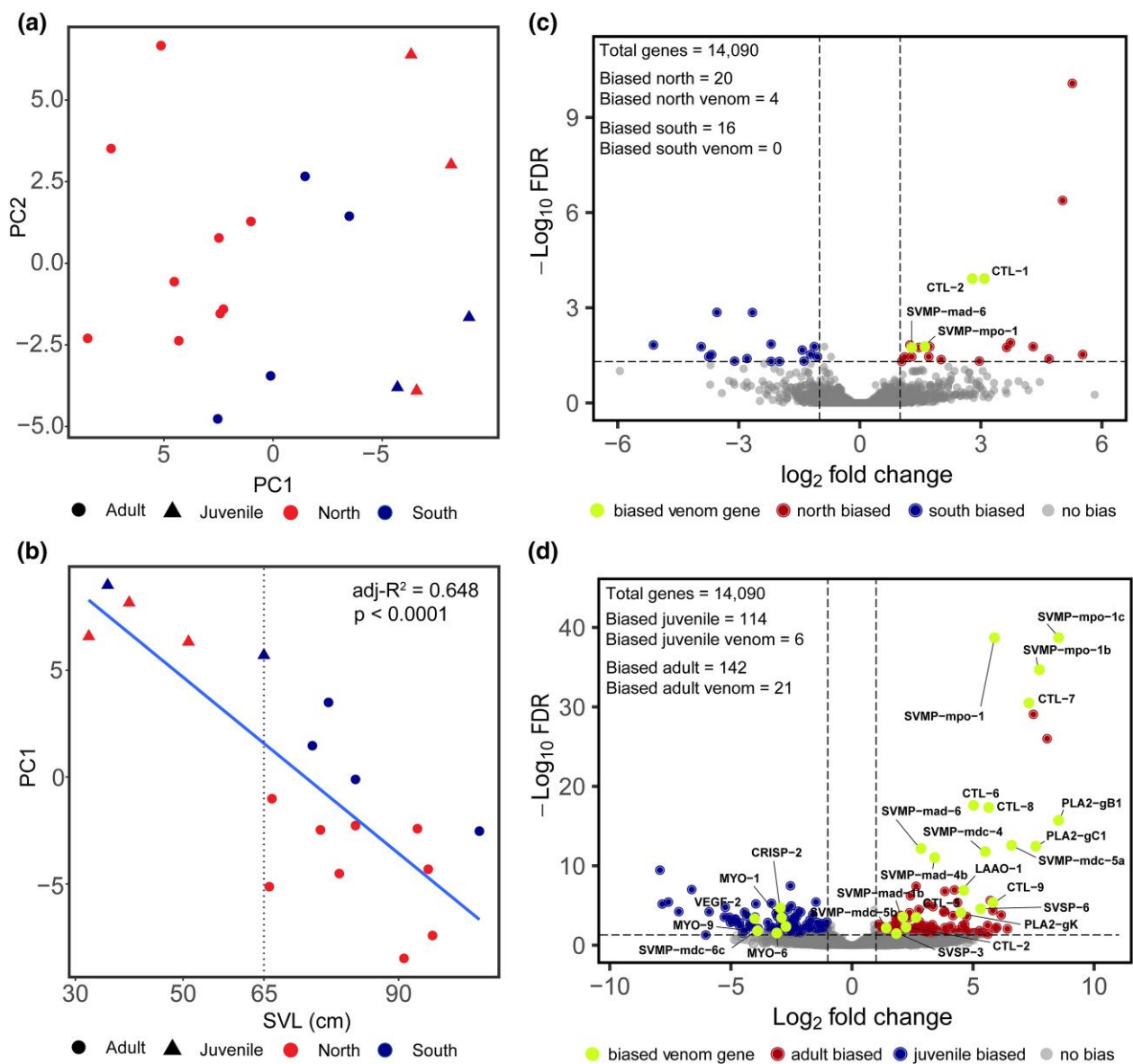


Fig. 3. Differential venom expression across life history and geographic space in *C. ruber*. a) Principal Component Analysis of venom-gland transcriptome DESEQ2 normalized count data, and b) Regression of Principal Component 1 (PC1) with SVL. Dotted line at 65 cm SVL shows the cut-off used for age class designation. Proportion of variance accounted for in PC1 and PC2 was 31% and 13%, respectively. c-d) Volcano plots of differential expression calculated from DESEQ2 between populations c) and age classes d). Vertical dotted lines represent $LFC \geq 1$, and horizontal dotted line represents $\alpha \leq 0.05$. Green points in each plot denote significantly DE toxin transcripts, and their placement denotes group bias. SVL, snout-vent-length; BPP, bradykinin-potentiating peptide; CRISP, cytesine-rich secretory protein; CTL, C-type lectin; MYO, myotoxin; PLA₂, phospholipase A₂; SVMP, snake venom metalloproteinase; SVSP, snake venom serine proteinase.

$adj-R^2 = 0.30$), prey availability (NMDS2; $P = 0.010$; $adj-R^2 = 0.14$), and abiotic factors (Bioclim PC1; $P = 0.012$; $adj-R^2 = 0.10$) were the most significant predictors of venom expression variation (Table 2).

Similarly, using read count estimations from Stringtie2 as the multivariate response variable, the full model, including all variables, was again significant ($P = 0.003$; $adj-R^2 = 0.66$; Table 3). The marginal model

($adj-R^2 = 0.62$) as determined from forward model selection differed slightly from the best model using HTSeq-count data as input; here, SVL ($P = 0.001$; $adj-R^2 = 0.44$), abiotic factors (Bioclim PC1; $P = 0.001$; $adj-R^2 = 0.12$), and nontoxin sequence variation (Nontoxin PCo1; $P = 0.020$; $adj-R^2 = 0.06$) were the most significant predictors of venom expression variation (Table 3).

Table 2 Results of the conditional RDA for venom-gland transcriptome normalized read count data from HTSeq-count as the response variable

	F	P-value	adj-R ²
Full Model	5.521	0.002	0.73
Marginal Model			0.54
SVL	8.32	0.003	0.30
Prey NMDS2	5.17	0.01	0.14
Bioclim PC1	4.49	0.012	0.10

Marginal model was identified using forward model selection on all explanatory variables. Results for all variables can be found in [supplementary table S3, Supplementary Material](#) online.

Table 3 Results of the conditional RDA for venom-gland transcriptome normalized read count data from stringtie2 as the response variable.

	F	P-value	adj-R ²
Full Model	4.29	0.003	0.66
Marginal Model			0.62
SVL	14.24	0.001	0.44
Bioclim PC1	5.38	0.001	0.12
Nontoxin PCo1	3.42	0.02	0.06

Marginal model was identified using forward model selection on all explanatory variables. Results for all variables can be found in [supplementary table S3, Supplementary Material](#) online.

Life History Best Explains Expression Evolution Across Individual Toxin Gene Families

We determined whether expression variation of the six most abundantly expressed toxin families (bradykinin-potentiating peptide [BPP], C-type lectin [CTL], Myotoxin, phospholipase A₂ [PLA₂], snake venom metalloproteinase [SVMP], snake venom serine proteinase [SVSP]) were significantly correlated with different explanatory variables. Variation across all toxin families, as identified in the marginal models, was significantly correlated with SVL (Table 4). Nontoxin sequence variation was also found to be a significant predictor of CTL, Myotoxin, and SVMP expression. Abiotic variation (Bioclim PC1) was the most significant predictor of PLA₂ expression variation. Prey was identified as a significant predictor of expression variation in BPP and SVSP toxin families, with prey availability (NMDS2) predicting BPP expression variation, and prey mean phylogenetic distance (MPD) predicting SVSP expression variation. See [supplementary table S3, Supplementary Material](#) online for detailed results of conditional RDAs for individual toxin families.

Discussion

Assembly and Annotation of Reference Quality *C. ruber* Genome

Genomic content of the reference genome assembly was similar to that of other snake assemblies (Vonk et al. 2013; Yin et al. 2016; Schield et al. 2019; Suryamohan

Table 4 Significant variables of the marginal models identified through forward model selection from conditional RDAs using the top six most abundantly expressed toxin families

Toxin Family	Marginal Model	P-value	adj-R ²
BPP	SVL	0.010	0.31
	Prey NMDS2	0.008	0.22
CTL	SVL	0.004	0.32
	Nontoxin PCo1	0.015	0.15
Myotoxin	SVL	0.004	0.34
	Nontoxin PCo1	0.039	0.13
PLA ₂	Bioclim PC1	0.001	0.38
	SVL	0.001	0.29
SVMP	SVL	0.007	0.27
SVSP	Nontoxin PCo1	0.013	0.18
	SVL	0.012	0.19
	Prey MPD	0.047	0.11

Results for all variables in each family can be found in [supplementary table S3, Supplementary Material](#) online.

et al. 2020; Li et al. 2021; Margres et al. 2021a; Westeen et al. 2023; Hogan et al. 2024). Notably, the *C. ruber* genome assembly displayed improved contiguity compared to several prior *Crotalus* assemblies, exhibiting a higher contig N50 and fewer total contigs compared to *C. tigris* (Margres et al. 2021a) and *C. viridis* (Schield et al. 2019). Overall, the accurate and contiguous reference-quality genome for *C. ruber* enabled us to robustly explore the effects of multiple evolutionary processes on venom evolution using reference-based genomic and transcriptomic analyses.

Population Genomics Reveals Two Genetically Distinct Populations with Unique Evolutionary Histories

We identified two genetically distinct populations separated by latitude with contact at ~26°N latitude near Loreto, BCS, MX (Fig. 2b), consistent with previous results (Harrington et al. 2018). Genetic differentiation between the two identified populations was extensive ($F_{ST} = 0.295\text{--}0.301$), with levels of fixation similar to that of highly genetically distinct populations of other North American vipers (Gibbs et al. 1997; Margres et al. 2019; Schmidt 2019). Reduced gene flow compared to expectations under a model of IBD was observed at the northeastern range edge near the Peninsular Ranges (Fig. 2d), which separate the California chaparral from the Sonoran Desert. The Sonoran Desert serves as a barrier to migration for many terrestrial organisms (Ernest et al. 2003; Brown et al. 2009), and for *C. ruber* (Greenberg 2002), the barrier likely exists due to climatic differences and competition with congeners such as its sister taxon, the Western Diamondback Rattlesnake (*C. atrox*; Alencar et al. 2016). Reduced gene flow was also observed near the Vizcaíno desert (Fig. 2d). Numerous species of the Baja region exhibit population differentiation occurring at the Vizcaíno desert (Riddle et al. 2000). Three hypotheses suggest that this

region may serve as a major barrier to migration in multiple organisms due to (i) a proposed ancient transpeninsular seaway that bisected the peninsula during the late Miocene to middle Pleistocene, (ii) isolation due to Pleistocene glacial–interglacial cycles, or (iii) differences in rainfall patterns between the peninsular regions (reviewed in Dolby et al. 2022). The Vizcaino desert region, however, functions only as a minor barrier to migration in *C. ruber*, at least relative to the Peninsular Ranges and subspecies boundary at ~26°N latitude (Fig. 2d). The deviation of *C. ruber* population structure from the patterns exhibited by other species (Riddle et al. 2000) was not associated with any apparent current or ancient topographic or geographic barriers to dispersal; rather, population structure has been proposed to be potentially linked with climatic fluctuations that occurred during the Pleistocene, resulting in temporary isolation of the two populations ~450–510 ka before present until secondary contact ~80 ka before present (Harrington et al. 2018). N_e in the northern and southern populations appeared to concordantly increase during the potential period of climate-driven isolation (~200–450 ka before present). At the time of purported secondary contact during the last glacial period (~80 ka before present), N_e decreased in the northern population while remaining relatively stable in the southern population (Fig. 2e). The observed differences in N_e between the two populations during the last glacial period suggests a pivotal role of climate-induced pressures on N_e and migration dynamics. Climate conditions were likely less favorable for snake survival in the northern range during glacial periods (Herbert et al. 2001), potentially driving the previously isolated northern population south and leading to decreased N_e and renewed contact with the southern population. Due to the limitations of PSMC in resolving more recent demographic histories, however, inferences of N_e near the present may not be inferred accurately (Liu and Fu 2015; Nadachowska-Brzyska et al. 2016; Patton et al. 2019). Additional biogeographic analyses and sampling would be needed to further explore the distinct evolutionary histories of the two populations identified here.

Venom Expression Differentiation Explained More by Ontogeny Than Genetic Population

Ontogenetic venom variation was much more pronounced than venom differentiation across populations. Indeed, age class explained ~22× more variance in venom proteomic composition and ~4× more variance in venom-gland transcriptome expression than population structure. The ontogenetic shift in venom expression occurred at ~65 cm SVL (supplementary fig. S3, Supplementary Material online) with continued variance throughout the life history of an individual, similar to other *Crotalus* species (Schonour et al. 2020). Differential expression of individual genes revealed

patterns of increased expression in SVMP and CTL toxin families in adults and the northern population and increased expression of myotoxins in juveniles. Myotoxins are small, basic peptides that induce physiologic tetanus of skeletal muscles, particularly in mice, and likely play an important role in subduing prey (Brenes et al. 1987; Mackessy et al. 2003; Mackessy 2021). SVMPs are a diverse family of large catabolic enzymes capable of causing severe damage to common structural proteins, inducing hemorrhage, and may aid in prey digestion (Kini and Koh 2016; Slagboom et al. 2017; Mackessy 2021). Variable ontogenetic and geographic expression of SVMPs and myotoxins is observed in multiple *Crotalus* species (Straight et al. 1991; Margres et al. 2015b; Smith et al. 2023), and such variation may be due to adaptive evolution. Adaptive differences may be produced by changes in prey preference at different life-history stages (Mushinsky et al. 1982) or optimal foraging strategy that promotes faster growth rates and reduces time spent in more vulnerable size classes (Werner and Gilliam 1984; Klauber 1997). For example, the production of large toxin enzymes such as SVMPs may be more metabolically costly (Mackessy 1988), leading to limited expression in juveniles. Although the precise mechanism remains unknown, the venom phenotype was significantly variable across age classes with only a limited number of toxins exhibiting differential expression across populations, suggesting that changes in venom expression due to maturity may have greater ecological implications (i.e. differences in prey size and/or species) compared to changes across populations.

Venom Variation Across Space Explained Primarily by Ontogeny with Significant but Reduced Effects of Other Selective Pressures and Neutral Processes

Venom Variation Best Explained by Snake Size

Conditional redundancy analysis integrating snake size, environmental factors, prey availability, and prey phylogenetic distance revealed that snake size (i.e. ontogeny) best predicted multivariate venom expression variation, regardless of which read count estimation method was employed, consistent with our venom analyses described above. Similar to geographic venom variation, ontogenetic venom variation is commonly attributed to selection (Andrade and Abe 1999; Gibbs et al. 2011; Webber et al. 2016; Cipriani et al. 2017). Snakes, as gape limited predators, may select prey at different life-history stages (Shine 1991); therefore, the venom phenotype may adaptively shift as size increases to more effectively subdue and/or digest different, larger prey species (Margres et al. 2015b). Variable efficacy of adult and juvenile venom in differing prey items is observed in multiple snake species (Mackessy 1988; Andrade and Abe 1999; Margres et al. 2016b; Cipriani et al. 2017; Borja et al. 2018), suggesting that ontogenetic venom

variation is often adaptive; however, the potential for neutral ontogenetic variation in snake venom has yet to be explored. Ontogeny may simply reflect developmental constraints which prevent the expression of otherwise beneficial traits or genes due to undeveloped key features or pathways (Gould and Lewontin 1979; Fernandez-Lorenzo et al. 1999; Barton and Boege 2017). Indeed, similar to other rattlesnakes (Margres et al. 2015b; Schonour et al. 2020; Hogan et al. 2024), we found that juvenile *C. ruber* venoms were simpler than adult venoms, with many more toxins upregulated in adults relative to juveniles (Fig. 3e). Despite the current lack of understanding on developmental constraints in snake venom, a better comprehension of the regulatory architecture underlying ontogenetic venom variation (Hogan et al. 2024) will enable future venom studies to incorporate such constraints into analyses of venom ontogeny.

Environmental differences also significantly explained venom expression variation using both read count estimation methods, consistent with previous work in other venomous snake species (Strickland et al. 2018; Margres et al. 2021b; Siqueira-Silva et al. 2021). Overall, variation in annual temperature and temporal fluctuations in temperature were the most important environmental factors (supplementary table S4, Supplementary Material online; PC1). Snakes further north experience cooler overall temperatures and greater annual temperature fluctuations compared to snakes in the south which experience consistently warmer temperatures throughout the year. Climatic factors such as temperature have been found to influence snake feeding behavior and prey preferences (Vincent and Mori 2008) which may in turn favor increased or decreased expression of certain toxin families that lead to more efficient feeding in particular climates. As described above, large toxin enzymes may aid in digestion; therefore, increased expression of these enzymes may be beneficial for snakes attempting to consume prey in cooler climates. Large enzymes such as SVMPs were more highly expressed in venoms from the northern population (Fig. 3c), suggesting a potential correlation between expression of putatively digestion-aiding toxin enzymes and cooler temperatures. Alternatively, environmental abiotic factors may have more accurately captured changes in prey availability across geographic space (see below), suggesting that venom expression variation corresponded with environmentally induced changes in prey availability. More detailed dietary analysis and toxicity measurements of different venoms in different prey under varying environmental conditions (e.g. assays conducted under different temperatures) would be needed to disentangle biotic and abiotic contributions to venom evolution.

Differences in prey availability were identified as significant within the marginal model using HTSeq-count derived data. Here, the significance of prey was primarily associated

with an increase in prey availability at the northern range edge compared to individuals found throughout the Baja California Peninsula (supplementary table S5, Supplementary Material online; NMDS2). Venom composition and variation is frequently associated with differences in prey availability among populations (Daltry et al. 1996; Barlow et al. 2009; Gibbs and Mackessy 2009; Holding et al. 2016; Margres et al. 2017a; Smiley-Walters et al. 2017; Robinson et al. 2021; Smith et al. 2023), and variation in the number of available prey species between *C. ruber* populations appeared to contribute, in part, to venom evolution. Variables of prey availability and prey mean phylogenetic distance (MPD) within our model, however, assumed (i) that all *C. ruber* would consume a given prey item if present within its geographic location, and (ii) all prey are equally abundant at each location. We acknowledge that these assumptions ignore ontogenetic changes in prey preference and/or geographic variation in prey abundance (Andrade and Abe 1999; Mackessy et al. 2006; Dugan and Hayes 2012; Cipriani et al. 2017). Additional diet information, including precise characterization of changes in prey composition across life-history stages and variation in abundance for each prey species across space, would be necessary to confirm size/geographic-induced dietary constraints or preferences here.

Lastly, nontoxin sequence variation was identified as a significant predictor of multivariate venom expression variation with read count estimation from stringtie2. Although it was the weakest predictor of venom expression variation ($\text{adj-}R^2 = 0.06$) compared to ontogeny, abiotic factors, and biotic factors, its presence in the marginal model suggested that neutral evolutionary processes minimally explain some variation in the overall venom phenotype. Therefore, neutral evolutionary processes may have a diminished yet still significant impact on venom evolution. Significance of nontoxin sequence variation within the model, however, may be potentially confounded by strong population structure (Fig. 2; Holding et al. 2018); such population structure may have been the product of geographically limited dispersal and genetic drift, and/or may be due to selective pressures causing reduced immigrant fitness (Garant et al. 2007). Still, results of the marginal model suggested that neutral sequence variation, our proxy for neutral evolutionary processes, significantly explained some variation in the overall venom phenotype.

Although both read-count methods identified SVL as the most significant predictor of venom expression variation, the other significant predictors and their contributions to the model varied between the two methods. Specifically, nontoxin sequence variation was only a significant predictor for all toxins when using StringTie2 estimates; however, it was also a significant predictor across three specific toxin families (CTL, SVMP, and myotoxin) when using

HTSeq-counts (Table 4). The significance of nontoxin sequence variation across both read-count methods provided confidence that the result was robust to any potential biases across methods. Why such differences occurred is not immediately clear, but varying sensitivities of the methods to different aspects of the data or inherent differences in how these methods process read counts were suspected (See Materials and Methods). Further evaluation of each method, potentially including additional datasets and validation of findings through complementary approaches, would be necessary to better understand these discrepancies.

Life History and Differing Secondary Factors Independently Contribute to Individual Toxin Family Evolution

Individual components of a complex trait like venom, such as specific toxin gene families, may evolve independently (Casewell et al. 2011, 2020; Schield et al. 2022); certain toxin families may play a more important role in specific aspects of feeding such as subduing, tracking, or digesting prey (Mackessy 2021), leading to unique evolutionary trajectories from different evolutionary mechanisms. For example, prey resistance to certain toxins or toxin families (Holding et al. 2016; Margres et al. 2017a; Gibbs et al. 2020; Robinson et al. 2021) may lead to variable expression of those toxins, whereas other toxins may evolve in response to abiotic conditions such as temperature (Tsai et al. 2003; Strickland et al. 2018; Margres et al. 2021b).

We tested whether variation across individual toxin families was best explained by distinct factors compared to multivariate venom expression variation. SVL was identified in the marginal models of all toxin families individually, further demonstrating the significance of ontogenetically induced venom variation in *C. ruber*. Variation in three of the toxin families (SVMP, CTL, myotoxin) was also significantly correlated with nontoxin sequence variation in addition to SVL (Table 4), suggesting that neutral evolutionary processes may contribute to variation across highly expressed toxin families of the venom phenotype. The relationship, however, may have been confounded by strong population structure (see above). Variation in the PLA₂ family was more significantly associated with environmental factors, particularly temperature, than SVL. Correlation between PLA₂ expression and environmental factors, especially those related to temperature, has been found in other Viperidae species (Tsai et al. 2003; Strickland et al. 2018; Margres et al. 2021b) and may be associated with temperature-driven variation in snake feeding behavior, prey availability, and/or prey preference (Vincent and Mori 2008). Consistent correlation observed across multiple species strongly implies a link between PLA₂ expression and environmental factors. Prey availability and prey phylogenetic distance was identified as a significant predictor of

expression variation across the BPP and SVSP toxin families, suggesting that the evolution of these families may be strongly linked with prey-induced selective pressures.

The inclusion of snake size in the marginal models for all of the most abundantly expressed toxin families was concordant with patterns of venom expression variation, highlighting the importance of life history in shaping venom evolution in *C. ruber*. However, variation of secondary factors identified in the marginal models across multiple toxin families, such as BPPs, SVSPs, and PLA₂s, prompts further investigation into (i) why certain toxin families exhibit distinct putative selection pressures, and (ii) whether these toxin families exhibit similar patterns across multiple species.

Conclusion

We sequenced and assembled the genome of *C. ruber*, characterized range-wide genetic and venom differentiation, and robustly explored the underlying factors associated with venom expression evolution, including neutral evolutionary processes. Venom variation was most significantly and overwhelmingly predicted by snake size; variation across life history may be the result of selection due to differences in prey and/or optimal foraging strategies (Adriaens et al. 2001; Hintz and Lonzarich 2018) or neutral mechanisms such as developmental constraints (Fernandez-Lorenzo et al. 1999; Barton and Boege 2017). Additional information on changes in diet preference across life history, functional data of venom toxicity in these prey, and characterization of the regulatory architecture underlying venom expression differentiation across age classes (e.g. Hogan et al. 2024) is needed to further explore the ultimate and proximate mechanisms driving ontogenetic venom variation in *C. ruber*. Although we also found that venom variation was significantly associated with abiotic and biotic factors, neutral patterns explained some variation in the venom phenotype and minimally warrant consideration and inclusion in future models.

By incorporating proxies for neutral and adaptive processes into a singular statistical framework, our study robustly shows the pivotal role of adaptive evolution in snake venoms, consistent with decades of research (Daltry et al. 1996; Sasa 1999; Mackessy et al. 2003; Sanz et al. 2006; Barlow et al. 2009; Vonk et al. 2013; Holding et al. 2016, 2018, 2021; Cipriani et al. 2017; Margres et al. 2017a; Smiley-Walters et al. 2017; Strickland et al. 2018; Davies and Arbuckle 2019; Arbuckle 2020; Casewell et al. 2020; Schonour et al. 2020; Margres et al. 2021b; Siqueira-Silva et al. 2021; Mason et al. 2022; Rao et al. 2022; Schield et al. 2022; Smith et al. 2023). However, several of these previous studies did not adequately account for neutral processes, providing reduced confidence in adaptive interpretations. We acknowledge

that our findings are based on the analysis of a single species and trait, and neutral processes may play a larger role in shaping phenotypic variation in other species and biological traits crucial to fitness and survival (Wright 1931; Nei 2005; Ho et al. 2017). Consequently, accounting for the influence of neutral evolutionary processes remains critical when investigating the forces producing trait variation, particularly within species. Our findings, together with those of others (e.g. Aird et al. 2017; Hague et al. 2020), underscore the necessity of considering the complexity of evolutionary processes when investigating phenotypic evolution.

Supplementary Material

Supplementary material is available at *Genome Biology and Evolution* online.

Acknowledgments

We would like to thank Sofía Alejandra Salinas Amézquita, Brandon La Forest, and Jacob Loyacano for their help with sampling as well as Ricardo Ramírez Chaparro for his help with sampling and providing photos. We would also like to thank A. Carl Whittington at the Florida State University BIO CORE Analytical Facility for assisting with RP-HPLC.

Author Contributions

S.R.H. and M.J.M. conceived and designed the study. All authors contributed to data collection and/or generation. S.R.H. and M.A.B. analyzed data. S.R.H. led writing with input from all coauthors.

Funding

This work was supported by the National Geographic Society (NGS-91224R-21) awarded to M.J.M., J.L.S., M.B., G.C.-G., A.R.R., C.L.P., and H.F.-C., the National Science Foundation Graduate Research Fellowship Program grant no. 2136515 awarded to S.R.H. and grant no. 1842493 awarded to M.A.B., the University of South Florida Graduate Research Fellowship awarded to S.R.H., the American Museum of Natural History Theodore Roosevelt Memorial Fund awarded to M.J.M., the National Science Foundation (DEB 1638879 and DEB 1822417) to C.L.P., the University of South Alabama College of Arts and Sciences Research and Scholarly Development funds to J.L.S., the Brigham Young University College of Life Sciences to P.B.F. and S.R.H., and the University of South Florida to M.J.M.

Conflict of interest

The authors declare no competing interests.

Data Availability

The data underlying this article are available in its online [supplementary material](#) and the National Center for Biotechnology Information (NCBI). All sequencing data generated in the study were submitted to NCBI under BioProject (PRJNA1051499). Accession numbers can be found in [supplementary table S6, Supplementary Material](#) online. Metadata are provided in [supplementary tables S1, S6, and S7, Supplementary Material](#) online. Ecological data were obtained from publicly available databases and all analytical softwares are publicly available.

Literature Cited

- Adriaens D, Aerts P, Verraes W. Ontogenetic shift in mouth opening mechanisms in a catfish (Clariidae, Siluriformes): a response to increasing functional demands. *J Morph.* 2001;247(3):197–216. [https://doi.org/10.1002/\(ISSN\)1097-4687](https://doi.org/10.1002/(ISSN)1097-4687).
- Aird SD, Arora J, Barua A, Qiu L, Terada K, Mikheyev AS. Population genomic analysis of a pitviper reveals microevolutionary forces underlying venom chemistry. *Genome Biol Evol.* 2017;9(10):2640–2649. <https://doi.org/10.1093/gbe/evx199>.
- Alape-Girón A, Sanz L, Escolano J, Flores-Díaz M, Madrigal M, Sasa M, Calvete JJ. Snake venomomics of the lancehead pitviper *Bothrops asper*: geographic, individual, and ontogenetic variations. *J Proteome Res.* 2008;7(8):3556–3571. <https://doi.org/10.1021/pr800332p>.
- Alencar LRV, Quental TB, Graziotin FG, Alfaro ML, Martins M, Venzon M, Zaher H. Diversification in vipers: phylogenetic relationships, time of divergence and shifts in speciation rates. *Mol Phylogenet Evol.* 2016;105(1055-7903):50–62. <https://doi.org/10.1016/j.ympev.2016.07.029>.
- Alexander HJ, Taylor JS, Wu SS-T, Breden F. Parallel evolution and vicariance in the guppy (*Poecilia reticulata*) over multiple spatial and temporal scales. *Evolution.* 2006;60(11):2352–2369. <https://doi.org/10.1111/evo.2006.60.issue-11>.
- Alonge M, Lebeigle L, Kirsche M, Jenike K, Ou S, Aganezov S, Wang X, Lippman ZB, Schatz MC, Soyk S. Automated assembly scaffolding using RagTag elevates a new tomato system for high-throughput genome editing. *Genome Biol.* 2022;23(1):258. <https://doi.org/10.1186/s13059-022-02823-7>.
- Anders S, Huber W. Differential expression analysis for sequence count data. *Genome Biol.* 2010;11(10):R106. <https://doi.org/10.1186/gb-2010-11-10-r106>.
- Anders S, Pyl PT, Huber W. HTSeq—a Python framework to work with high-throughput sequencing data. *Bioinformatics.* 2015;31(2):166–169. <https://doi.org/10.1093/bioinformatics/btu638>.
- Andrade DV, Abe AS. Relationship of venom ontogeny and diet in *Bothrops*. *Herpetologica.* 1999;55(2):200–204.
- Arbuckle K. From molecules to macroevolution: venom as a model system for evolutionary biology across levels of life. *Toxicon.* 2020;6(2590-1710):100034. <https://doi.org/10.1016/j.toxcx.2020.100034>.
- Astashyn A, Tvedte ES, Sweeney D, Sapojnikov V, Bouk N, Joukov V, Mozes E, Strobe PK, Sylla PM, Wagner L, et al. Rapid and sensitive detection of genome contamination at scale with FCS-GX. *Gen Bio.* 2024;25(1):60. <https://doi.org/10.1186/s13059-024-03198-7>.
- Barlow A, Pook CE, Harrison RA, Wüster W. Coevolution of diet and prey-specific venom activity supports the role of selection in

- snake venom evolution. *Proc Natl Acad Sci*. 2009;276(1666):2443–2449. <https://doi.org/10.1098/rspb.2009.0048>.
- Barton KE, Boege K. Future directions in the ontogeny of plant defence: understanding the evolutionary causes and consequences. *Ecol Lett*. 2017;20(4):403–411. <https://doi.org/10.1111/ele.2017.20.issue-4>.
- Borja M, Neri-Castro E, Pérez-Morales R, Strickland JL, Ponce-López R, Parkinson CL, Espinosa-Fematt J, Sáenz-Mata J, Flores-Martínez E, Alagón A, et al. Ontogenetic change in the venom of Mexican black-tailed rattlesnakes (*Crotalus molossus nigrescens*). *Toxins*. 2018;10(12):501. <https://doi.org/10.3390/toxins10120501>.
- Bradburd GS, Coop GM, Ralph PL. Inferring continuous and discrete population genetic structure across space. *Genetics*. 2018;210(1):33–52. <https://doi.org/10.1534/genetics.118.301333>.
- Brandies P, Peel E, Hogg CJ, Belov K. The value of reference genomes in the conservation of threatened species. *Genes*. 2019;10(11):846. <https://doi.org/10.3390/genes10110846>.
- Brenes F, Gutiérrez JM, Lomonte B. Immunohistochemical demonstration of the binding of Bothrops asper myotoxin to skeletal muscle sarcolemma. *Toxicol*. 1987;25(5):574–577. [https://doi.org/10.1016/0041-0101\(87\)90294-7](https://doi.org/10.1016/0041-0101(87)90294-7).
- Brodie ED, Brodie ED. Tetrodotoxin resistance in garter snakes: an evolutionary response of predators to dangerous prey. *Evolution*. 1990;44(3):651–659. <https://doi.org/10.1111/evo.1990.44.issue-3>.
- Brodie ED, Feldman CR, Hanifin CT, Motychak JE, Mulcahy DG, Williams BL, Brodie ED. Parallel arms races between garter snakes and newts involving tetrodotoxin as the phenotypic interface of coevolution. *J Chem Ecol*. 2005;31(2):343–356. <https://doi.org/10.1007/s10886-005-1345-x>.
- Brodie ED, Ridenhour BJ, Brodie ED. The evolutionary response of predators to dangerous prey: hotspots and coldspots in the geographic mosaic of coevolution between garter snakes and newts. *Evolution*. 2002;56(10):2067–2082. <https://doi.org/10.1111/j.0014-3820.2002.tb00132.x>.
- Broecker WS, Hemming S. Climate swings come into focus. *Science*. 2001;294(5550):2308–2309. <https://doi.org/10.1126/science.1068389>.
- Brown SK, Hull JM, Updike DR, Fain SR, Ernest HB. Black bear population genetics in California: signatures of population structure, competitive release, and historical translocation. *J Mammalogy*. 2009;90(5):1066–1074. <https://doi.org/10.1644/08-MAMM-A-193.1>.
- Bush J, Webster C, Wegryzn J, Simon C, Wilcox E, Khan R, Weisz D, Dudchenko O, Aiden EL, Frandsen P. Chromosome-level genome assembly and annotation of a periodical cicada species: *magicicada septendecula*. *Gen Bio Evo*. 2024;16(1):evae001. <https://doi.org/10.1093/gbe/evae001>.
- Capblancq T, Forester BR. Redundancy analysis: a Swiss Army Knife for landscape genomics. *Methods Ecol Evol*. 2021;12(12):2298–2309. <https://doi.org/10.1111/mee3.v12.12>.
- Casewell NR, Jackson TNW, Laustsen AH, Sunagar K. Causes and consequences of snake venom variation. *Trends in Pharm Sci*. 2020;41(8):570–581. <https://doi.org/10.1016/j.tips.2020.05.006>.
- Casewell NR, Wagstaff SC, Harrison RA, Renjifo C, Wüster W. Domain loss facilitates accelerated evolution and neofunctionalization of duplicate snake venom metalloproteinase toxin genes. *Mol Biol Evol*. 2011;28(9):2637–2649. <https://doi.org/10.1093/molbev/msr091>.
- Casewell NR, Wagstaff SC, Wüster W, Cook DAN, Bolton FMS, King SI, Pla D, Sanz L, Calvete JJ, Harrison RA. Medically important differences in snake venom composition are dictated by distinct post-genomic mechanisms. *Proc Natl Acad Sci*. 2014;111(25):9205–9210. <https://doi.org/10.1073/pnas.1405484111>.
- Castoe TA, Spencer CL, Parkinson CL. Phylogeographic structure and historical demography of the western diamondback rattlesnake (*Crotalus atrox*): a perspective on North American desert biogeography. *Mol Phylogenet Evol*. 2007;42(1):193–212. <https://doi.org/10.1016/j.ympev.2006.07.002>.
- Cheng H, Concepcion GT, Feng X, Zhang H, Li H. Haplotype-resolved de novo assembly using phased assembly graphs with hifiasm. *Nat Methods*. 2021;18(2):170–175. <https://doi.org/10.1038/s41592-020-01056-5>.
- Cingolani P, Platts A, Wang LL, Coon M, Nguyen T, Wang L, Land SJ, Lu X, Ruden DM. A program for annotating and predicting the effects of single nucleotide polymorphisms, SnpEff. *Fly (Austin)*. 2012;6(2):80–92. <https://doi.org/10.4161/fly.19695>.
- Cipriani V, Debono J, Goldenberg J, Jackson TNW, Arbuckle K, Dobson J, Koludarov I, Li B, Hay C, Dunstan N, et al. Correlation between ontogenetic dietary shifts and venom variation in Australian brown snakes (*Pseudonaja*). *Comp Biochem Physiol*. 2017;197(1532-0456):53–60. <https://doi.org/10.1016/j.cbpc.2017.04.007>.
- Clark RW, Tangco S, Barbour MA. Field video recordings reveal factors influencing predatory strike success of free-ranging rattlesnakes (*Crotalus* spp.). *Anim Behav*. 2012;84(1):183–190. <https://doi.org/10.1016/j.anbehav.2012.04.029>.
- Dale RK, Pedersen BS, Quinlan AR. Pybedtools: a flexible Python library for manipulating genomic datasets and annotations. *Bioinformatics*. 2011;27(24):3423–3424. <https://doi.org/10.1093/bioinformatics/btr539>.
- Daltry JC, Wüster W, Thorpe RS. Diet and snake venom evolution. *Nature*. 1996;379(6565):537–540. <https://doi.org/10.1038/379537a0>.
- Danecek P, Auton A, Abecasis G, Albers CA, Banks E, DePristo MA, Handsaker RE, Lunter G, Marth GT, Sherry ST, et al. 1000 Genomes Project Analysis Group. The variant call format and VCFtools. *Bioinformatics*. 2011;27(15):2156–2158. <https://doi.org/10.1093/bioinformatics/btr330>.
- Darwin C. On the origin of species by means of natural selection, or the preservation of favoured races in the struggle for life. *Albemarle Street: John Murray*; 1859.
- Davies E-L, Arbuckle K. Coevolution of snake venom toxic activities and diet: evidence that ecological generalism favours toxicological diversity. *Toxins*. 2019;11(12):711. <https://doi.org/10.3390/toxins11120711>.
- Dickson LB, Jiolle D, Minard G, Moltini-Conclois I, Volant S, Ghazlane A, Bouchier C, Ayala D, Paupy C, Moro CV, et al. Carryover effects of larval exposure to different environmental bacteria drive adult trait variation in a mosquito vector. *Sci Adv*. 2017;3(8):e1700585. <https://doi.org/10.1126/sciadv.1700585>.
- Dolby GA, Bennett SE, Dorsey RJ, Stokes MF, Riddle BR, Lira-Noriega A, Munguia-Vega A, Wilder BT. Integrating earth–life systems: a genomic approach. *Trends Ecol Evol*. 2022;37(4):371–384. <https://doi.org/10.1016/j.tree.2021.12.004>.
- Dugan EA, Hayes WK. Diet and feeding ecology of the red diamond rattlesnake, *Crotalus ruber* (Serpentes: Viperidae). *Herpetologica*. 2012;68(2):203–217. <https://doi.org/10.1655/HERPETOLOGICA-D-11-00008.1>.
- Durban J, Sanz L, Trevisan-Silva D, Neri-Castro E, Alagón A, Calvete JJ. Integrated venomomics and venom gland transcriptome analysis of juvenile and adult Mexican rattlesnakes *Crotalus simus*, *C. tzabcan*, and *C. culminatus* revealed miRNA-modulated ontogenetic shifts. *J Proteome Res*. 2017;16(9):3370–3390. <https://doi.org/10.1021/acs.jproteome.7b00414>.
- Eaton DAR, Overcast I. Ipyrad: interactive assembly and analysis of RADseq datasets. *Bioinformatics*. 2020;36(8):2592–2594. <https://doi.org/10.1093/bioinformatics/btz966>.
- Ernest HB, Boyce WM, Bleich VC, May B, Stiver SJ, Torres SG. Genetic structure of mountain lion (*Puma concolor*) populations in California. *Cons Gen*. 2003;4(3):353–366. <https://doi.org/10.1023/A:1024069014911>.

- Fernandez-Lorenzo JL, Rigueiro A, Ballester A. Polyphenols as potential markers to differentiate juvenile and mature chestnut shoot cultures. *Tree Physiol.* 1999;19(7):461–466. <https://doi.org/10.1093/treephys/19.7.461>.
- Fisher RA. 086: the distribution of gene ratios for rare mutations. 1930. Fraser HB. Gene expression drives local adaptation in humans. *Genome Res.* 2013;23(7):1089–1096. <https://doi.org/10.1101/gr.152710.112>.
- Garant D, Forde SE, Hendry AP. The multifarious effects of dispersal and gene flow on contemporary adaptation. *Func Ecol.* 2007;21(3):434–443. <https://doi.org/10.1111/fec.2007.21.issue-3>.
- Gibbs HL, Mackessy SP. Functional basis of a molecular adaptation: prey-specific toxic effects of venom from *Sistrurus rattlesnakes*. *Toxicon.* 2009;53(6):672–679. <https://doi.org/10.1016/j.toxicon.2009.01.034>.
- Gibbs HL, Prior KA, Weatherhead PJ, Johnson G. Genetic structure of populations of the threatened eastern massasauga rattlesnake, *Sistrurus c. catenatus*: evidence from microsatellite DNA markers. *Mol Ecol.* 1997;6(12):1123–1132. <https://doi.org/10.1046/j.1365-294X.1997.00284.x>.
- Gibbs HL, Rossiter W. Rapid evolution by positive selection and gene gain and loss: PLA2 venom genes in closely related *Sistrurus* rattlesnakes with divergent diets. *J Mol Evol.* 2008;66(2):151–166. <https://doi.org/10.1007/s00239-008-9067-7>.
- Gibbs HL, Sanz L, Calvete JJ. Snake population venomics: proteomics-based analyses of individual variation reveals significant gene regulation effects on venom protein expression in *Sistrurus* rattlesnakes. *J Mol Evol.* 2009;68(2):113–125. <https://doi.org/10.1007/s00239-008-9186-1>.
- Gibbs HL, Sanz L, Chiucchi JE, Farrell TM, Calvete JJ. Proteomic analysis of ontogenetic and diet-related changes in venom composition of juvenile and adult Dusky Pigmy rattlesnakes (*Sistrurus miliarius barbouri*). *J Proteomics.* 2011;74(10):2169–2179. <https://doi.org/10.1016/j.jprot.2011.06.013>.
- Gibbs HL, Sanz L, Pérez A, Ochoa A, Hassinger AT, Holding ML, Calvete JJ. The molecular basis of venom resistance in a rattlesnake-squirrel predator-prey system. *Mol Ecol.* 2020;29(15):2871–2888. <https://doi.org/10.1111/mec.v29.15>.
- Gompel N, Prud'homme B, Wittkopp PJ, Kassner VA, Carroll SB. Chance caught on the wing: cis-regulatory evolution and the origin of pigment patterns in *Drosophila*. *Nature.* 2005;433(7025):481–487. <https://doi.org/10.1038/nature03235>.
- Gould SJ, Lewontin RC. The spandrels of San Marco and the Panglossian paradigm: a critique of the adaptationist programme. *Proc Natl Acad Sci.* 1979;205(1161):581–598. <https://doi.org/10.1098/rspb.1979.0086>.
- Grant PR, Grant BR. Unpredictable evolution in a 30-year study of Darwin's finches. *Science.* 2002;296(5568):707–711. <https://doi.org/10.1126/science.1070315>.
- Greenberg DB. The ecology of movement and site selection in desert rattlesnakes (*Crotalus mitchellii* and *Crotalus ruber*) of the southwestern United States. [Ph.D. thesis]. University of California, Santa Barbara, United States – California; 2002.
- Gremme G, Steinbiss S, Kurtz S. GenomeTools: a comprehensive software library for efficient processing of structured genome annotations. *Transactions Comp Bio Bioinformatics.* 2013;10(3):645–656. <https://doi.org/10.1109/TCBB.2013.68>.
- Grismer LL. Amphibians and reptiles of Baja California, including its Pacific islands and the islands in the Sea of Cortés. Berkeley (CA): University of California Press; 2002.
- Gruber B, Unmack PJ, Berry OF, Georges A. Dartr: an R package to facilitate analysis of SNP data generated from reduced representation genome sequencing. *Mol Ecol Resour.* 2018;18(3):691–699. <https://doi.org/10.1111/men.2018.18.issue-3>.
- Gu Z, Gu L, Eils R, Schlesner M, Brors B. Circlize implements and enhances circular visualization in R. *Bioinformatics.* 2014;30(19):2811–2812. <https://doi.org/10.1093/bioinformatics/btu393>.
- Hague MTJ, Stokes AN, Feldman CR, Brodie Jr ED, Brodie III ED. The geographic mosaic of arms race coevolution is closely matched to prey population structure. *Evol Lett.* 2020;4(4):317–332. <https://doi.org/10.1002/evl3.184>.
- Hanifin CT, Brodie Jr ED, Brodie III ED. Phenotypic mismatches reveal escape from Arms-Race coevolution. *PLOS Biol.* 2008;6(3):e60. <https://doi.org/10.1371/journal.pbio.0060060>.
- Harrington SM, Hollingsworth BD, Higham TE, Reeder TW. Pleistocene climatic fluctuations drive isolation and secondary contact in the red diamond rattlesnake (*Crotalus ruber*) in Baja California. *J Biogeogr.* 2018;45(1):64–75. <https://doi.org/10.1111/jbi.2018.45.issue-1>.
- Herbert TD, Schuffert JD, Andreasen D, Heusser L, Lyle M, Mix A, Ravelo AC, Stott LD, Herguera JC. Collapse of the California current during glacial maxima linked to climate change on land. *Science.* 2001;293(5527):71–76. <https://doi.org/10.1126/science.1059209>.
- Hester MW, Mendelsohn IA, McKee KL. Species and population variation to salinity stress in *Panicum hemitomon*, *Spartina patens*, and *Spartina alterniflora*: morphological and physiological constraints. *Env Exp Botany.* 2001;46(3):277–297. [https://doi.org/10.1016/S0098-8472\(01\)00100-9](https://doi.org/10.1016/S0098-8472(01)00100-9).
- Hijmans RJ, Cameron SE, Parra JL, Jarvis A. Very high resolution interpolated climate surfaces for global land areas. *Intl J Clim.* 2005;25(15):1965–1978. [https://doi.org/10.1002/\(ISSN\)1097-0088](https://doi.org/10.1002/(ISSN)1097-0088).
- Hintz WD, Lonzarich DG. Maximizing foraging success: the roles of group size, predation risk, competition, and ontogeny. *Ecosphere.* 2018;9(10):e02456. <https://doi.org/10.1002/ecs2.2456>.
- Ho W-C, Ohya Y, Zhang J. Testing the neutral hypothesis of phenotypic evolution. *Proc Natl Acad Sci.* 2017;114(46):12219–12224. <https://doi.org/10.1073/pnas.1710351114>.
- Hoekstra HE, Hirschmann RJ, Bunday RA, Insel PA, Crossland JP. A single amino acid mutation contributes to adaptive beach mouse color pattern. *Science.* 2006;313(5783):101–104. <https://doi.org/10.1126/science.1126121>.
- Hogan MP, Holding ML, Nystrom GS, Colston TJ, Bartlett DA, Mason AJ, Ellsworth SA, Rautsaw RM, Lawrence KC, Strickland JL, et al. The genetic regulatory architecture and epigenomic basis for age-related changes in rattlesnake venom. *Proc Natl Acad Sci.* 2024;121(16):e2313440121. <https://doi.org/10.1073/pnas.2313440121>.
- Holding ML, Biardi JE, Gibbs HL. Coevolution of venom function and venom resistance in a rattlesnake predator and its squirrel prey. *Proc Royal Soc.* 2016;283(1829):20152841. <https://doi.org/10.1098/rspb.2015.2841>.
- Holding ML, Margres MJ, Rokyta DR, Gibbs HL. Local prey community composition and genetic distance predict venom divergence among populations of the northern Pacific rattlesnake (*Crotalus oreganus*). *J Evo Bio.* 2018;31(10):1513–1528. <https://doi.org/10.1111/jeb.2018.31.issue-10>.
- Holding ML, Strickland JL, Rautsaw RM, Hofmann EP, Mason AJ, Hogan MP, Nystrom GS, Ellsworth SA, Colston TJ, Borja M, et al. Phylogenetically diverse diets favor more complex venoms in North American pitvipers. *Proc Natl Acad Sci.* 2021;118(17):e2015579118. <https://doi.org/10.1073/pnas.2015579118>.
- Jackson TNW, Fry BG. A tricky trait: applying the fruits of the “function debate” in the philosophy of biology to the “venom debate” in the science of toxinology. *Toxins.* 2016;8(9):263. <https://doi.org/10.3390/toxins8090263>.
- Jackson TNW, Koludarov I, Ali SA, Dobson J, Zdenek CN, Dashevsky D, Masci PP, Nouwens A, Josh P, Goldenberg J, et al. Rapid radiations

- and the race to redundancy: an investigation of the evolution of Australian elapid snake venoms. *Toxins* (Basel). 2016;8(11):309. <https://doi.org/10.3390/toxins8110309>.
- Johnson M, Zaretskaya I, Raytselis Y, Merezchuk Y, McGinnis S, Madden TL. NCBI BLAST: a better web interface. *Nuc Acid Res*. 2008;36(suppl_2):W5–W9. <https://doi.org/10.1093/nar/gkn201>.
- Jones P, Binns D, Chang H-Y, Fraser M, Li W, McAnulla C, McWilliam H, Maslen J, Mitchell A, Nuka G, et al. InterProScan 5: genome-scale protein function classification. *Bioinformatics*. 2014;30(9):1236–1240. <https://doi.org/10.1093/bioinformatics/btu031>.
- Juárez P, Comas I, González-Candelas F, Calvete JJ. Evolution of snake venom disintegrins by positive Darwinian selection. *Mol Biol Evol*. 2008;25(11):2391–2407. <https://doi.org/10.1093/molbev/msn179>.
- Kearse M, Moir R, Wilson A, Stones-Havas S, Cheung M, Sturrock S, Buxton S, Cooper A, Markowitz S, Duran C, et al. Geneious basic: an integrated and extendable desktop software platform for the organization and analysis of sequence data. *Bioinformatics*. 2012;28(12):1647–1649. <https://doi.org/10.1093/bioinformatics/bts199>.
- Keilwagen J, Hartung F, Grau J. GeMoMa: homology-based gene prediction utilizing intron position conservation and RNA-seq data. In: Kollmar M, editor. *Gene Prediction: Methods and Protocols*. Methods in Molecular Biology. New York (NY): Springer; 2019. p. 161–177.
- Keller SR, Sowell DR, Neiman M, Wolfe LM, Taylor DR. Adaptation and colonization history affect the evolution of clines in two introduced species. *New Phyt*. 2009;183(3):678–690. <https://doi.org/10.1111/nph.2009.183.issue-3>.
- Kembel SW, Cowan PD, Helmus MR, Cornwell WK, Morlon H, Ackerly DD, Blomberg SP, Webb CO. Picante: R tools for integrating phylogenies and ecology. *Bioinformatics*. 2010;26(11):1463–1464. <https://doi.org/10.1093/bioinformatics/btq166>.
- Kim D, Paggi JM, Park C, Bennett C, Salzberg SL. Graph-based genome alignment and genotyping with HISAT2 and HISAT-genotype. *Nat Biotechnol*. 2019;37(8):907–915. <https://doi.org/10.1038/s41587-019-0201-4>.
- Kimura M. Evolutionary rate at the molecular level. *Nature*. 1968;217(5129):624–626. <https://doi.org/10.1038/217624a0>.
- Kini RM, Koh CY. Metalloproteases affecting blood coagulation, fibrinolysis and platelet aggregation from snake venoms: definition and nomenclature of interaction sites. *Toxins*. 2016;8(10):284. <https://doi.org/10.3390/toxins8100284>.
- Klauber LM. *Rattlesnakes: their habits, life histories, and influence on mankind*. Berkeley (CA): University of California Press; 1997.
- Konczal M, Babik W, Radwan J, Sadowska ET, Koteja P. Initial molecular-level response to artificial selection for increased aerobic metabolism occurs primarily through changes in gene expression. *Mol Biol Evol*. 2015;32(6):1461–1473. <https://doi.org/10.1093/molbev/msv038>.
- Kumar S, Stecher G, Suleski M, Hedges SB. TimeTree: a resource for timelines, timetrees, and divergence times. *Mol Biol Evol*. 2017;34(7):1812–1819. <https://doi.org/10.1093/molbev/msx116>.
- Lande R. Natural selection and random genetic drift in phenotypic evolution. *Evolution*. 1976;30(2):314–334. <https://doi.org/10.2307/2407703>.
- Langmead B, Salzberg SL. Fast gapped-read alignment with Bowtie 2. *Nat Methods*. 2012;9(4):357–359. <https://doi.org/10.1038/nmeth.1923>.
- Li H, Durbin R. Inference of human population history from individual whole-genome sequences. *Nature*. 2011;475(7357):493–496. <https://doi.org/10.1038/nature10231>.
- Li A, Wang J, Sun K, Wang S, Zhao X, Wang T, Xiong L, Xu W, Qiu L, Shang Y, et al. Two reference-quality sea snake genomes reveal their divergent evolution of adaptive traits and venom systems. *Mol Biol Evol*. 2021;38(11):4867–4883. <https://doi.org/10.1093/molbev/msab212>.
- Liu Q. Variation partitioning by partial redundancy analysis (RDA). *Environmetrics*. 1997;8(2):75–85. [https://doi.org/10.1002/\(ISSN\)1099-095X](https://doi.org/10.1002/(ISSN)1099-095X).
- Liu X, Fu Y-X. Exploring population size changes using SNP frequency spectra. *Nat Genet*. 2015;47(5):555–559. <https://doi.org/10.1038/ng.3254>.
- Liu X, Zhao J, Xue L, Zhao T, Ding W, Han Y, Ye H. A comparison of transcriptome analysis methods with reference genome. *BMC Genomics*. 2022;23(1):232. <https://doi.org/10.1186/s12864-022-08465-0>.
- Love MI, Huber W, Anders S. Moderated estimation of fold change and dispersion for RNA-seq data with DESeq2. *Genome Biol*. 2014;15(12):550. <https://doi.org/10.1186/s13059-014-0550-8>.
- Mackessy SP. Venom ontogeny in the Pacific rattlesnakes *Crotalus viridis helleri* and *C. v. oregonus*. *Copeia*. 1988;1988(1):92–101. <https://doi.org/10.2307/1445927>.
- Mackessy SP. *Handbook of venoms and toxins of reptiles*. Boca Raton (FL): CRC Press; 2021.
- Mackessy SP, Sixberry NM, Heyborne WH, Fritts T. Venom of the brown treesnake, *Boiga irregularis*: ontogenetic shifts and taxa-specific toxicity. *Toxicon*. 2006;47(5):537–548. <https://doi.org/10.1016/j.toxicon.2006.01.007>.
- Mackessy SP, Williams K, Ashton KG. Ontogenetic variation in venom composition and diet of *Crotalus oregonus concolor*: a case of venom paedomorphosis? *Copeia*. 2003;2003(4):769–782. <https://doi.org/10.1643/HA03-037.1>.
- Margres MJ, Aronow K, Loyacano J, Rokyta DR. The venom-gland transcriptome of the eastern coral snake (*Micrurus fulvius*) reveals high venom complexity in the intragenomic evolution of venoms. *BMC Genom*. 2013;14(1):531. <https://doi.org/10.1186/1471-2164-14-531>.
- Margres MJ, Bigelow AT, Lemmon EM, Lemmon AR, Rokyta DR. Selection to increase expression, not sequence diversity, precedes gene family origin and expansion in rattlesnake venom. *Genetics*. 2017b;206(3):1569–1580. <https://doi.org/10.1534/genetics.117.202655>.
- Margres MJ, McGivern JJ, Seavy M, Wray KP, Facente J, Rokyta DR. Contrasting modes and tempos of venom expression evolution in two snake species. *Genetics*. 2015a;199(1):165–176. <https://doi.org/10.1534/genetics.114.172437>.
- Margres MJ, McGivern JJ, Wray KP, Seavy M, Calvin K, Rokyta DR. Linking the transcriptome and proteome to characterize the venom of the eastern diamondback rattlesnake (*Crotalus adamanteus*). *J Proteomics*. 2014;96(1874-3919):145–158. <https://doi.org/10.1016/j.jprot.2013.11.001>.
- Margres MJ, Patton A, Wray KP, Hassinger ATB, Ward MJ, Lemmon EM, Lemmon AR, Rokyta DR. Tipping the scales: the migration–selection balance leans toward selection in snake venoms. *Mol Biol Evol*. 2019;36(2):271–282. <https://doi.org/10.1093/molbev/msy207>.
- Margres MJ, Rautsaw RM, Strickland JL, Mason AJ, Schramer TD, Hofmann EP, Stiers E, Ellsworth SA, Nystrom GS, Hogan MP, et al. The Tiger Rattlesnake genome reveals a complex genotype underlying a simple venom phenotype. *Proc Natl Acad Sci*. 2021a;118(4):e2014634118. <https://doi.org/10.1073/pnas.2014634118>.
- Margres MJ, Walls R, Suntravat M, Lucena S, Sánchez EE, Rokyta DR. Functional characterizations of venom phenotypes in the eastern diamondback rattlesnake (*Crotalus adamanteus*) and evidence for expression-driven divergence in toxic activities among populations. *Toxicon*. 2016b;119(0041-0101):28–38. <https://doi.org/10.1016/j.toxicon.2016.05.005>.

- Margres MJ, Wray KP, Hassinger ATB, Ward MJ, McGivern JJ, Moriarty Lemmon E, Lemmon AR, Rokyta DR. Quantity, not quality: rapid adaptation in a polygenic trait proceeded exclusively through expression differentiation. *Mol Biol Evol.* 2017a;34(12):3099–3110. <https://doi.org/10.1093/molbev/msx231>.
- Margres MJ, Wray KP, Sanader D, McDonald PJ, Trumbull LM, Patton AH, Rokyta DR. Varying intensities of introgression obscure incipient venom-associated speciation in the timber rattlesnake (*Crotalus horridus*). *Toxins.* 2021b;13(11):782. <https://doi.org/10.3390/toxins13110782>.
- Margres MJ, Wray KP, Seavy M, McGivern JJ, Herrera ND, Rokyta DR. Expression differentiation is constrained to low-expression proteins over ecological timescales. *Genetics.* 2016a;202(1):273–283. <https://doi.org/10.1534/genetics.115.180547>.
- Margres MJ, Wray KP, Seavy M, McGivern JJ, Sanader D, Rokyta DR. Phenotypic integration in the feeding system of the eastern diamond-back rattlesnake (*Crotalus adamanteus*). *Mol Ecol.* 2015b;24(13):3405–3420. <https://doi.org/10.1111/mec.2015.24.issue-13>.
- Mason AJ, Holding ML, Rautsaw RM, Rokyta DR, Parkinson CL, Gibbs HL. Venom gene sequence diversity and expression jointly shape diet adaptation in pitvipers. *Mol Biol Evol.* 2022;39(4):msac082. <https://doi.org/10.1093/molbev/msac082>.
- Mason AJ, Margres MJ, Strickland JL, Rokyta DR, Sasa M, Parkinson CL. Trait differentiation and modular toxin expression in palm-pitvipers. *BMC Genomics.* 2020;21(1):147. <https://doi.org/10.1186/s12864-020-6545-9>.
- Massey DJ, Calvete JJ, Sánchez EE, Sanz L, Richards K, Curtis R, Boesen K. Venom variability and envenoming severity outcomes of the *Crotalus scutulatus scutulatus* (Mojave rattlesnake) from Southern Arizona. *J Proteomics.* 2012;75(9):2576–2587. <https://doi.org/10.1016/j.jprot.2012.02.035>.
- McKenna A, Hanna M, Banks E, Sivachenko A, Cibulskis K, Kernytsky A, Garimella K, Altshuler D, Gabriel S, Daly M, et al. The genome analysis toolkit: a mapReduce framework for analyzing next-generation DNA sequencing data. *Genome Res.* 2010;20(9):1297–1303. <https://doi.org/10.1101/gr.107524.110>.
- Modahl CM, Mukherjee AK, Mackessy SP. An analysis of venom ontogeny and prey-specific toxicity in the Monocled Cobra (*Naja kaouthia*). *Toxicon.* 2016;119(0041-0101):8–20. <https://doi.org/10.1016/j.toxicon.2016.04.049>.
- Müller R, Kaj I, Mugal CF. A nearly neutral model of molecular signatures of natural selection after change in population size. *Genome Biol Evol.* 2022;14(1759-6653):5–evac058. <https://doi.org/10.1093/gbe/evac058>.
- Mushinsky HR, Hebrard JJ, Vodopich DS. Ontogeny of water snake foraging ecology. *Ecology.* 1982;63(6):1624–1629. <https://doi.org/10.2307/1940102>.
- Nadachowska-Brzyska K, Burri R, Smeds L, Ellegren H. Psmc analysis of effective population sizes in molecular ecology and its application to black-and-white ficedula flycatchers. *Mol Ecol.* 2016;25(5):1058–1072. <https://doi.org/10.1111/mec.2016.25.issue-5>.
- Nei M. Selectionism and neutralism in molecular evolution. *Mol Biol Evol.* 2005;22(12):2318–2342. <https://doi.org/10.1093/molbev/msi242>.
- Nevo E. Genetic variation in natural populations: patterns and theory. *Theo Pop Biol.* 1978;13(1):121–177. [https://doi.org/10.1016/0040-5809\(78\)90039-4](https://doi.org/10.1016/0040-5809(78)90039-4).
- Ohta T. Slightly deleterious mutant substitutions in evolution. *Nature.* 1973;246(5428):96–98. <https://doi.org/10.1038/246096a0>.
- Oksanen J, Blanchet FG, Friendly M, Kindt R, Legendre P, McGlenn D, Minchin P, O'Hara RB, Simpson G, Solymos P, et al. *Vegan community ecology Package Version 2.5-7* November 2020. 2020.
- Patton AH, Margres MJ, Stahlke AR, Hendricks S, Lewallen K, Hamede RK, Ruiz-Aravena M, Ryder O, McCallum HI, Jones ME, et al. Contemporary demographic reconstruction methods are robust to genome assembly quality: a case study in Tasmanian devils. *Mol Biol Evol.* 2019;36(12):2906–2921. <https://doi.org/10.1093/molbev/msz191>.
- Pertea M, Pertea GM, Antonescu CM, Chang T-C, Mendell JT, Salzberg SL. StringTie enables improved reconstruction of a transcriptome from RNA-seq reads. *Nat Biotechnol.* 2015;33(3):290–295. <https://doi.org/10.1038/nbt.3122>.
- Petkova D, Novembre J, Stephens M. Visualizing spatial population structure with estimated effective migration surfaces. *Nat Genet.* 2016;48(1):94–100. <https://doi.org/10.1038/ng.3464>.
- Pla D, Sanz L, Quesada-Bernat S, Villalta M, Baal J, Chowdhury MAW, León G, Gutiérrez JM, Kuch U, Calvete JJ. Phylogenomics of *daboia russelii* across the Indian subcontinent. Bioactivities and comparative in vivo neutralization and in vitro third-generation antivenomics of antivenoms against venoms from India, Bangladesh and Sri Lanka. *J Proteomics.* 2019;207(1876-7737):103443. <https://doi.org/10.1016/j.jprot.2019.103443>.
- Pozas-Ocampo IF, Carbajal-Saucedo A, Gatica-Colima AB, Cordero-Tapia A, Arnaud-Franco G. Toxicological comparison of *Crotalus ruber lucasensis* venom from different ecoregions of the Baja California Peninsula. *Toxicon.* 2020;187(0041-0101):111–115. <https://doi.org/10.1016/j.toxicon.2020.08.029>.
- Pozo G, Albuja-Quintana M, Larreátegui L, Gutiérrez B, Fuentes N, Alfonso-Cortés F, Torres MDL. First whole-genome sequence and assembly of the Ecuadorian brown-headed spider monkey (*Ateles fusciceps fusciceps*), a critically endangered species, using Oxford Nanopore Technologies. *G3.* 2024;14(3):jkae014. <https://doi.org/10.1093/g3journal/jkae014>.
- Purcell S, Neale B, Todd-Brown K, Thomas L, Ferreira MAR, Bender D, Maller J, Sklar P, de Bakker PIW, Daly MJ, et al. PLINK: a tool set for whole-genome association and population-based linkage analyses. *Am J Hum Genet.* 2007;81(3):559–575. <https://doi.org/10.1086/519795>.
- Putri GH, Anders S, Pyl PT, Pimanda JE, Zanini F. Analysing high-throughput sequencing data in Python with HTSeq 2.0. *Bioinformatics.* 2022;38(10):2943–2945. <https://doi.org/10.1093/bioinformatics/btac166>.
- Rao W-Q, Kalogeropoulos K, Allentoft ME, Gopalakrishnan S, Zhao W-N, Workman CT, Knudsen C, Jiménez-Mena B, Seneci L, Mousavi-Derazmahalleh M, et al. The rise of genomics in snake venom research: recent advances and future perspectives. *Gigascience.* 2022;11(2047-217X):giac024. <https://doi.org/10.1093/gigascience/giac024>.
- Rautsaw RM, Hofmann EP, Margres MJ, Holding ML, Strickland JL, Mason AJ, Rokyta DR, Parkinson CL. Intraspecific sequence and gene expression variation contribute little to venom diversity in sidewinder rattlesnakes (*Crotalus cerastes*). *Proc Natl Acad Sci.* 2019;286(1906):20190810. <https://doi.org/10.1098/rspb.2019.0810>.
- Rhie A, Walenz BP, Koren S, Phillippy AM. Merqury: reference-free quality, completeness, and phasing assessment for genome assemblies. *Genome Biol.* 2020;21(1):245. <https://doi.org/10.1186/s13059-020-02134-9>.
- Riddle BR, Hafner DJ, Alexander LF, Jaeger JR. Cryptic vicariance in the historical assembly of a Baja California peninsular desert biota. *Proc Natl Acad Sci.* 2000;97(26):14438–14443. <https://doi.org/10.1073/pnas.250413397>.
- Robinson KE, Holding ML, Whitford MD, Saviola AJ, Yates III JR, Clark RW. Phenotypic and functional variation in venom and venom resistance of two sympatric rattlesnakes and their prey. *J Evo Biol.* 2021;34(9):1447–1465. <https://doi.org/10.1111/jeb.v34.9>.
- Rohlf RV, Harrigan P, Nielsen R. Modeling gene expression evolution with an extended Ornstein–Uhlenbeck process accounting for

- within-species variation. *Mol Biol Evol.* 2014;31(1):201–211. <https://doi.org/10.1093/molbev/mst190>.
- Rokyta DR, Lemmon AR, Margres MJ, Aronow K. The venom-gland transcriptome of the eastern diamondback rattlesnake (*Crotalus adamanteus*). *BMC Genom.* 2012;13(1):312. <https://doi.org/10.1186/1471-2164-13-312>.
- Rokyta DR, Margres MJ, Calvin K. Post-transcriptional mechanisms contribute little to phenotypic variation in snake venoms. *G3.* 2015;5(11):2375–2382. <https://doi.org/10.1534/g3.115.020578>.
- Rokyta DR, Margres MJ, Ward MJ, Sanchez EE. The genetics of venom ontogeny in the eastern diamondback rattlesnake (*Crotalus adamanteus*). *PeerJ.* 2017;5(2167-8359):e3249. <https://doi.org/10.7717/peerj.3249>.
- Rokyta DR, Wray KP, Margres MJ. The genesis of an exceptionally lethal venom in the timber rattlesnake (*Crotalus horridus*) revealed through comparative venom-gland transcriptomics. *BMC Genomics.* 2013;14(1):394. <https://doi.org/10.1186/1471-2164-14-394>.
- Rotenberg D, Bamberger ES, Kochva E. Studies on ribonucleic acid synthesis in the venom glands of *Vipera palaestinae* (Ophidia, Reptilia). *Biochem J.* 1971;121(4):609–612. <https://doi.org/10.1042/bj1210609>.
- Salamov AA, Solovyev VV. Ab initio gene finding in *Drosophila* genomic DNA. *Genome Res.* 2000;10(4):516–522. <https://doi.org/10.1101/gr.10.4.516>.
- Sanz L, Gibbs HL, Mackessy SP, Calvete JJ. Venom proteomes of closely related *Sistrurus* rattlesnakes with divergent diets. *J Proteome Res.* 2006;5(9):2098–2112. <https://doi.org/10.1021/pr0602500>.
- Sasa M. Diet and snake venom evolution: can local selection alone explain intraspecific venom variation?. *Toxicon.* 1999;37(2):249–252. author reply 253–260. [https://doi.org/10.1016/S0041-0101\(98\)00121-4](https://doi.org/10.1016/S0041-0101(98)00121-4).
- Schild DR, Card DC, Hales NR, Perry BW, Pasquesi GM, Blackmon H, Adams RH, Corbin AB, Smith CF, Ramesh B, et al. The origins and evolution of chromosomes, dosage compensation, and mechanisms underlying venom regulation in snakes. *Genome Res.* 2019;29(4):590–601. <https://doi.org/10.1101/gr.240952.118>.
- Schild DR, Perry BW, Adams RH, Holding ML, Nikolakis ZL, Gopalan SS, Smith CF, Parker JM, Meik JM, DeGiorgio M, et al. The roles of balancing selection and recombination in the evolution of rattlesnake venom. *Nat Ecol Evol.* 2022;6(9):1367–1380. <https://doi.org/10.1038/s41559-022-01829-5>.
- Schiffels S, Durbin R. Inferring human population size and separation history from multiple genome sequences. *Nat Genet.* 2014;46(8):919–925. <https://doi.org/10.1038/ng.3015>.
- Schmidt DA. Patterns of population structure and genetic diversity among Western Rattlesnakes (*Crotalus oreganus*) in the Pacific Northwest. [Ph.D. thesis]. University of British Columbia; 2019.
- Schonour RB, Huff EM, Holding ML, Claunch NM, Ellsworth SA, Hogan MP, Wray K, McGivern J, Margres MJ, Colston TJ, et al. Gradual and discrete ontogenetic shifts in rattlesnake venom composition and assessment of hormonal and ecological correlates. *Toxins.* 2020;12(10):659. <https://doi.org/10.3390/toxins12100659>.
- Senji Laxme RR, Khochare S, de Souza HF, Ahuja B, Suranse V, Martin G, Whitaker R, Sunagar K. Beyond the ‘big four’: venom profiling of the medically important yet neglected Indian snakes reveals disturbing antivenom deficiencies. *PLoS Negl Trop Dis.* 2019;13(12):e0007899. <https://doi.org/10.1371/journal.pntd.0007899>.
- Serra F, Becher V, Dopazo H. Neutral theory predicts the relative abundance and diversity of genetic elements in a broad array of eukaryotic genomes. *PLoS One.* 2013;8(6):e63915. <https://doi.org/10.1371/journal.pone.0063915>.
- Shine R. Why do larger snakes eat larger prey items? *Func Ecol.* 1991;5(4):493–502. <https://doi.org/10.2307/2389631>.
- Sim SB, Corpuz RL, Simmonds TJ, Geib SM. HiFiAdapterFilter, a memory efficient read processing pipeline, prevents occurrence of adapter sequence in PacBio HiFi reads and their negative impacts on genome assembly. *BMC Genomics.* 2022;23(1):157. <https://doi.org/10.1186/s12864-022-08375-1>.
- Simão FA, Waterhouse RM, Ioannidis P, Kriventseva EV, Zdobnov EM. BUSCO: Assessing genome assembly and annotation completeness with single-copy orthologs. *Bioinformatics.* 2015;31(19):3210–3212. <https://doi.org/10.1093/bioinformatics/btv351>.
- Siqueira-Silva T, de Lima LAG, Chaves-Silveira J, Amado TF, Naipauer J, Riul P, Martinez PA. Ecological and biogeographic processes drive the proteome evolution of snake venom. *Global Eco Biogeog.* 2021;30(10):1978–1989. <https://doi.org/10.1111/geb.v30.10>.
- Slagboom J, Kool J, Harrison RA, Casewell NR. Haemotoxic snake venoms: their functional activity, impact on snakebite victims and pharmaceutical promise. *Br J Haematol.* 2017;177(6):947–959. <https://doi.org/10.1111/bjh.2017.177.issue-6>.
- Smiley-Walters SA, Farrell TM, Gibbs HL. Evaluating local adaptation of a complex phenotype: reciprocal tests of pigmy rattlesnake venoms on treefrog prey. *Oecologia.* 2017;184(4):739–748. <https://doi.org/10.1007/s00442-017-3882-8>.
- Smith CF, Nikolakis ZL, Ivey K, Perry BW, Schield DR, Balchan NR, Parker J, Hansen KC, Saviola AJ, Castoe TA, et al. Snakes on a plain: biotic and abiotic factors determine venom compositional variation in a wide-ranging generalist rattlesnake. *BMC Biol.* 2023;21(1):136. <https://doi.org/10.1186/s12915-023-01626-x>.
- Straight RC, Glenn JL, Wolt TB, Wolfe MC. Regional differences in content of small basic peptide toxins in the venoms of *Crotalus adamanteus* and *Crotalus horridus*. *Comp Biochem Physiol.* 1991;100(1):51–58. [https://doi.org/10.1016/0305-0491\(91\)90083-P](https://doi.org/10.1016/0305-0491(91)90083-P).
- Straight RC, Glenn JL, Wolt TB, Wolfe MC. North-south regional variation in phospholipase a activity in the venom of *Crotalus ruber*. *Comp Biochem Physiol.* 1992;103(3):635–639. [https://doi.org/10.1016/0305-0491\(92\)90382-2](https://doi.org/10.1016/0305-0491(92)90382-2).
- Strickland JL, Smith CF, Mason AJ, Schield DR, Borja M, Castañeda-Gaytán G, Spencer CL, Smith LL, Trápaga A, Bouzid NM, et al. Evidence for divergent patterns of local selection driving venom variation in Mojave Rattlesnakes (*Crotalus scutulatus*). *Sci Rep.* 2018;8(1):17622. <https://doi.org/10.1038/s41598-018-35810-9>.
- Summers K, Cronin TW, Kennedy T. Variation in spectral reflectance among populations of *Dendrobates pumilio*, the strawberry poison frog, in the Bocas del Toro Archipelago, Panama. *J Biogeog.* 2003;30(1):35–53. <https://doi.org/10.1046/j.1365-2699.2003.00795.x>.
- Suryamohan K, Krishnankutty SP, Guillory J, Jevit M, Schröder MS, Wu M, Kuriakose B, Mathew OK, Perumal RC, Koludarov I, et al. The Indian cobra reference genome and transcriptome enables comprehensive identification of venom toxins. *Nat Genet.* 2020;52(1):106–117. <https://doi.org/10.1038/s41588-019-0559-8>.
- Templ M, Hron K, Filzmoser P, Facevicova K, Kynclova P, Walach J, Pintar V, Chen J, Miksova D, Meindl B, et al. robCompositions: compositional data analysis. 2023.
- Terhorst J, Kamm JA, Song YS. Robust and scalable inference of population history from hundreds of unphased whole genomes. *Nat Genet.* 2017;49(2):303–309. <https://doi.org/10.1038/ng.3748>.
- Tsai I-H, Wang Y-M, Chen Y-H. Variations of phospholipases A₂ in the geographic venom samples of pitvipers. *J Toxicology.* 2003;22(4):651–662. <https://doi.org/10.1081/TXR-120026919>.
- van den Wollenberg AL. Redundancy analysis an alternative for canonical correlation analysis. *Psychometrika.* 1977;42(2):207–219. <https://doi.org/10.1007/BF02294050>.
- Vincent SE, Mori A. Determinants of feeding performance in free-ranging pit-vipers (*Viperidae*: *Ovophis okinawensis*): key roles for

- head size and body temperature. *Bio J Linnean Soc.* 2008;93(1): 53–62. <https://doi.org/10.1111/j.1095-8312.2007.00928.x>.
- Vonk FJ, Casewell NR, Henkel CV, Heimberg AM, Jansen HJ, McCleary RJR, Kerckamp HME, Vos RA, Guerreiro I, Calvete JJ, et al. The king cobra genome reveals dynamic gene evolution and adaptation in the snake venom system. *Proc Natl Acad Sci.* 2013;110(51):20651–20656. <https://doi.org/10.1073/pnas.1314702110>.
- Webber MM, Jezkova T, Rodríguez-Robles JA. Feeding ecology of sidewinder rattlesnakes, *Crotalus cerastes* (Viperidae). *Herpetologica.* 2016;72(4):324–330. <https://doi.org/10.1655/Herpetologica-D-15-00031.1>.
- Werner EE, Gilliam JF. The ontogenetic niche and species interactions in size-structured populations. *Annual Rev Eco Syst.* 1984;15(1): 393–425. <https://doi.org/10.1146/ecolsys.1984.15.issue-1>.
- Westen EP, Escalona M, Holding ML, Beraut E, Fairbairn C, Marimuthu MPA, Nguyen O, Perri R, Fisher RN, Toffelmier E, et al. A genome assembly for the southern Pacific rattlesnake, *Crotalus oreganus helleri*, in the western rattlesnake species complex. *Journal of Heredity.* 2023;114(6):681–689. <https://doi.org/10.1093/jhered/esad045>.
- Williams BL, Brodie Jr ED, Brodie III ED. Coevolution of deadly toxins and predator resistance: self-assessment of resistance by garter snakes leads to behavioral rejection of toxic newt prey. *Herpetologica.* 2003;59(2):155–163. [https://doi.org/10.1655/0018-0831\(2003\)059\[0155:CODTAP\]2.0.CO;2](https://doi.org/10.1655/0018-0831(2003)059[0155:CODTAP]2.0.CO;2).
- Williams BL, Hanifin CT, Brodie ED, Brodie III ED. Tetrodotoxin affects survival probability of rough-skinned newts (*Taricha granulosa*) faced with TTX-resistant garter snake predators (*Thamnophis sirtalis*). *Chemoecology.* 2010;20(4):285–290. <https://doi.org/10.1007/s00049-010-0057-z>.
- Williams V, White J, Schwaner TD, Sparrow A. Variation in venom proteins from isolated populations of tiger snakes (*Notechis ater niger*, *N. scutatus*) in South Australia. *Toxicon.* 1988;26(11):1067–1075. [https://doi.org/10.1016/0041-0101\(88\)90205-X](https://doi.org/10.1016/0041-0101(88)90205-X).
- Wray KP, Margres MJ, Seavy M, Rokyta DR. Early significant ontogenetic changes in snake venoms. *Toxicon.* 2015;96(0041-0101): 74–81. <https://doi.org/10.1016/j.toxicon.2015.01.010>.
- Wright S. Evolution in mendelian populations. *Genetics.* 1931;16(2): 97–159. <https://doi.org/10.1093/genetics/16.2.97>.
- Wright S. Isolation by distance. *Genetics.* 1943;28(2):114. <https://doi.org/10.1093/genetics/28.2.114>.
- Yang Y, Servedio MR, Richards-Zawacki CL. Imprinting sets the stage for speciation. *Nature.* 2019;574(7776):99–102. <https://doi.org/10.1038/s41586-019-1599-z>.
- Yin W, Wang Z-J, Li Q-Y, Lian J-M, Zhou Y, Lu B-Z, Jin L-J, Qiu P-X, Zhang P, Zhu W-B, et al. Evolutionary trajectories of snake genes and genomes revealed by comparative analyses of five-pacer viper. *Nat Commun.* 2016;7(2041-1723):13107. <https://doi.org/10.1038/ncomms13107>.
- Zhang J. Neutral theory and phenotypic evolution. *Mol Biol Evol.* 2018;35(6):1327–1331. <https://doi.org/10.1093/molbev/msy065>.
- Zhao H-Y, Sun Y, Du Y, Li J-Q, Lv J-G, Qu Y-F, Lin L-H, Lin C-X, Ji X, Gao J-F. Venom of the annulated sea snake hydrophis cyanocinctus: a biochemically simple but genetically complex weapon. *Toxins.* 2021;13(8):548. <https://doi.org/10.3390/toxins13080548>.

Associate editor: Kirk Lohmueller